AJNR

Clinical Arterial Spin-Labeling MR Imaging to Screen for Typical and Atypical Neurodegenerative Disease in the New Era of Alzheimer Treatment

Kevin Lee, Meem Mahmud, Darby Marx, Weiye Yasen, Omna Sharma, Jana Ivanidze, Elcin Zan, Liangdong Zhou, Yi Li, Mony J. de Leon, Anna S. Nordvig and Gloria C. Chiang

AJNR Am J Neuroradiol published online 14 March 2024
http://www.ajnr.org/content/early/2024/03/14/ajnr.A8164

Published March 14, 2024 as 10.3174/ajnr.A8164

Clinical Arterial Spin-Labeling MR Imaging to Screen for Typical and Atypical Neurodegenerative Disease in the New Era of Alzheimer Treatment

Kevin Lee, Meem Mahmud, Darby Marx, Weiye Yasen, Omna Sharma, Jana Ivanidze, Elcin Zan, Liangdong Zhou, Yi Li, Mony J. de Leon, Anna S. Nordvig, and Gloria C. Chiang

ABSTRACT

SUMMARY: The clinical standard of care in the diagnosis of neurodegenerative diseases relies on [^{18}F] FDG-PET/CT or PET MR imaging. Limitations of FDG-PET include cost, the need for IV access, radiation exposure, and availability. Arterial spin-labeling MR imaging has been shown in research settings to be useful as a proxy for FDG-PET in differentiating Alzheimer disease from frontotemporal dementia. However, it is not yet widely used in clinical practice, except in cerebrovascular disease. Here, we present 7 patients, imaged with our routine clinical protocol with diverse presentations of Alzheimer disease and other neurodegenerative diseases, in whom arterial spin-labeling–derived reduced CBF correlated with hypometabolism or amyloid/tau deposition on PET. Our case series illustrates the clinical diagnostic utility of arterial spin-labeling MR imaging as a fast, accessible, and noncontrast screening tool for neurodegenerative disease. Arterial spin-labeling MR imaging can guide patient selection for subsequent PET or fluid biomarker work-up, as well as for possible therapy with antiamyloid monoclonal antibodies.

ABBREVIATIONS: AD = Alzheimer disease; ADLs = activities of daily living; ASL = arterial spin-labeling; CI = cognitive impairment; COVID-19 = coronavirus 2019; lvPPA = logopenic variant progressive aphasia; MCI = mild cognitive impairment; MoCA = Montreal Cognitive Assessment; PCA = posterior cortical atrophy

Neurodegenerative disease, of which Alzheimer disease (AD) is the most common, is the leading cause of dementia and manifests as progressive cognitive impairment (CI) along with a variety of other neurologic symptoms.[1] Standard-of-care MR imaging can exclude potentially treatable, structural causes of CI and can identify atrophy but lacks sensitivity and specificity. In the era of antiamyloid monoclonal antibody therapy for AD, identifying reliable and easily accessible diagnostic tools for neurodegenerative disease is of paramount importance.

FDG-PET is routinely used clinically to differentiate AD from other neurodegenerative diseases.[1] Recently, the Centers for Medicare and Medicaid Services decreased the restrictions on the coverage of amyloid PET, providing more access to patients seeking antiamyloid therapies.[2] However, both FDG and amyloid PET scans are costly, requiring IV access for radiotracer administration, radiation exposure, and proximity to a PET facility.

Arterial spin-labeling MR imaging (ASL-MR) is a noncontrast MR imaging technique that uses endogenous water in arterial blood for a qualitative and quantitative assessment of CBF.[3] Its utility as a surrogate measure of neuronal activity and metabolism on FDG-PET has been described in AD research settings, particularly at the group level;[4] however, it has thus far not been demonstrated in clinical practice.

We present 7 cases of neurodegenerative disease (6 with forms of AD) in which a clinical MR imaging protocol to evaluate cognitive impairment that included a 4.5-minute ASL MR image was effective at predicting findings on subsequent PET, even when structural imaging was not revealing. Full informed consent was obtained from all patients. We propose that ASL-MR could be a cost-effective AD screening and longitudinal follow-up tool.

CASE SERIES

Case 1: Early-Onset AD with Presenilin Mutation

A 57-year-old postmenopausal woman with a history of thyroid cancer and hyperlipidemia presented with slowly progressive short-term memory loss for 10–15 years, as well as anxiety and fatigue for 1–2 years. She was independent in activities of daily living (ADLs). Her father and 3 paternal siblings had onset of dementia at ages 50–60

Received November 8, 2023; accepted after revision January 3, 2024.

From the Weill Cornell Medical College (K.L., D.M., W.Y.), New York, New York; Department of Radiology (L.Z., Y.L., M.J.d.L., G.C.C.), Brain Health Imaging Institute, Department of Molecular Imaging and Therapeutics (J.I., E.Z.), and Department of Neurology (M.M., A.S.N.), Alzheimer's Disease and Memory Disorders Program, Weill Cornell Medicine, NewYork-Presbyterian Hospital, New York, New York; and Weill Cornell Medicine (O.S.), Qatar Foundation, Education City, Doha, Qatar.

G.C. Chiang and A.S. Nordvig contributed equally to this article.

This work was supported by National Institute of Neurological Disorders and Stroke NeuroNEXT Fellowship Award 5U24NS107168, National Institutes of Health/National Institute on Aging R01 AG068398, National Institutes of Health/National Institute on Aging R01 AG080011.

Please address correspondence to Kevin Lee, BS, c/o Gloria Chiang 525 E 68th St, Box 141, Starr 6 New York, NY 10065; e-mail: kel4009@med.cornell.edu; @GloriaChiangMD; @AnnaNordvig; @Kevin_Lee097

Indicates article with online supplemental data.

http://dx.doi.org/10.3174/ajnr.A8164

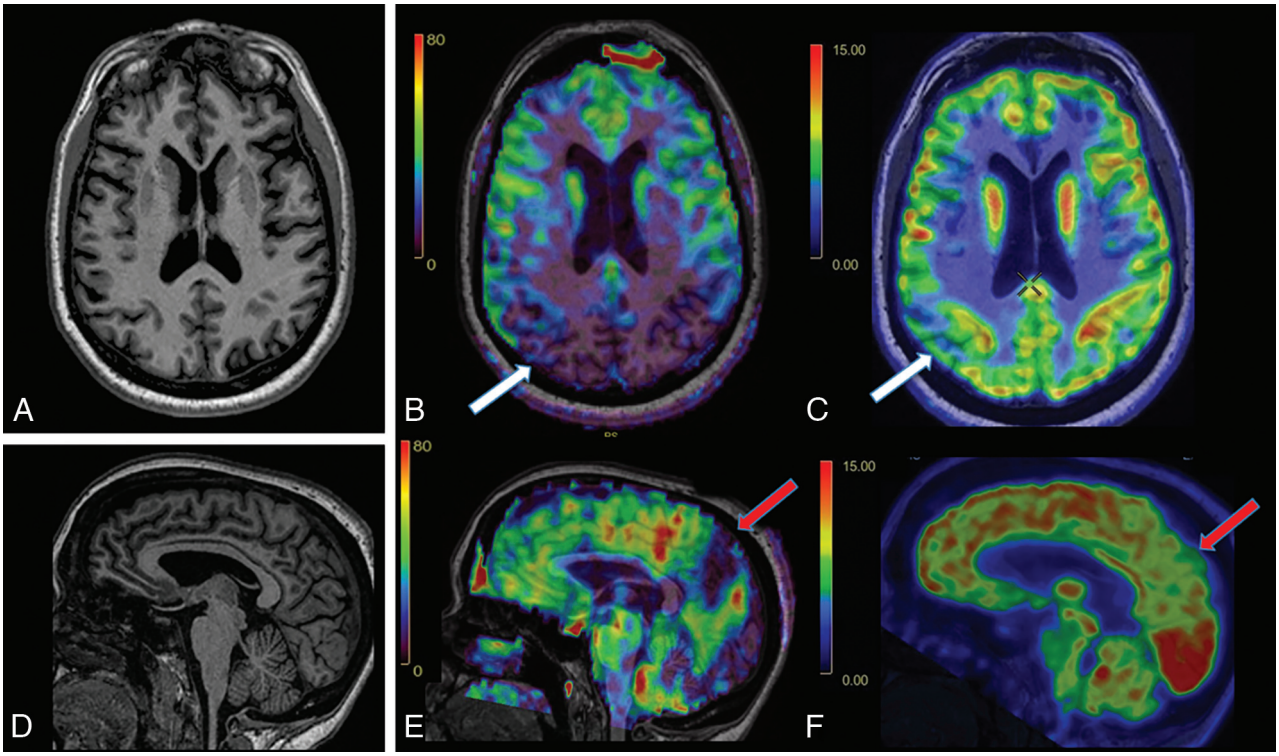

FIG 1. Early-onset AD with *presenilin* mutation. *A*, Axial 3D TI MPRAGE image shows mild generalized volume loss. Axial CBF image (*B*) and axial FDG-PET image (*C*) show more pronounced decreased CBF than FDG avidity in the bilateral parietal lobes, particularly on the right (*white arrow*), and temporal lobes (not pictured), suggestive of AD. *D*, Sagittal 3D TI MPRAGE image shows nonspecific volume loss. Sagittal CBF image (*E*) and sagittal FDG-PET image (*F*) show decreased CBF and FDG avidity in the precuneus (*red arrow*).

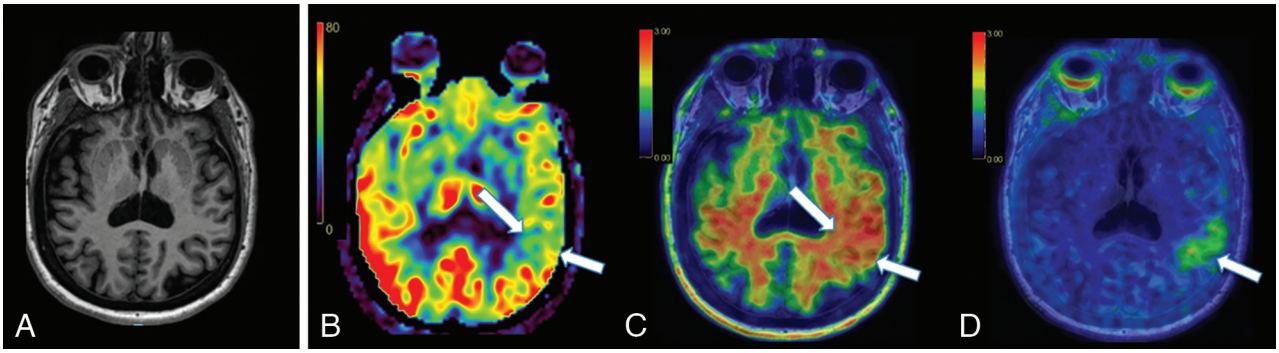

FIG 2. Early-onset AD and post-COVID brain fog. *A*, Axial 3D TI MPRAGE image shows mild volume loss, more prominent in the left hemisphere. *B*, Axial CBF image shows asymmetrically decreased CBF in the left temporoparietal junction (*white arrows*). *C*, Axial [^{18}F] florbetaben PET image shows asymmetric cortical deposition of β-amyloid (*white arrows*). *D*. Axial [^{18}F]-MK6240 tau PET shows focal cortical deposition of tau (*white arrows*), corresponding to the area of lowest CBF noted in *B* and β-amyloid deposition in *C*.

years. Two siblings were cognitively healthy. Neurologic assessment showed mild cognitive impairment (MCI), a Montreal Cognitive Assessment (MoCA) score of 16/30, and mild parietal drift. Serum labs were noncontributory. Structural MR imaging showed nonspecific mild volume loss. ASL-MR showed decreased bilateral temporoparietal CBF, including in the precuneus (Fig 1 and Online Supplemental Data); FDG-PET corresponded to these findings (Fig 1 and Online Supplemental Data). Amyloid PET revealed diffuse cortical amyloid deposition (Online Supplemental Data). Genetic testing revealed a heterozygous *PSEN1* mutation (c.617G>C hereditary autosomal dominant AD). The patient has been prescribed lecanemab.

Case 2: Early-Onset AD and Long COVID Brain Fog

A 53-year-old woman with pre-existing hypertension and seronegative presumed rheumatologic disease presented with "brain fog," insomnia, orthostasis, and headaches after mild coronavirus 2019 (COVID-19) infection. Following a COVID-19 vaccination, she developed Bell palsy and peripheral herpes simplex virus reactivation. She had previously worked full-time in a cognitively demanding position. Maternal family history was positive for AD onset around the age of 60. She had a MoCA score of 29/30, a Mini-Mental State Examination score of 30/30, and facial nerve findings of Bell palsy. The initial clinical diagnosis was post-COVID MCI, with worsened rheumatologic disease. However,

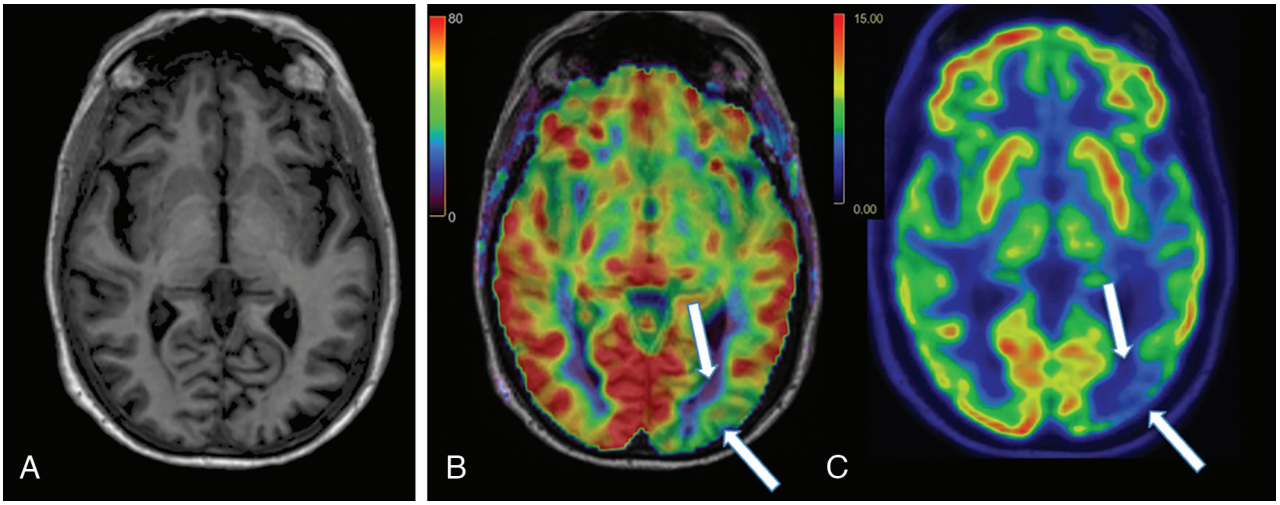

FIG 3. PCA, the "visual variant" of AD. *A*, Axial 3D T1 MPRAGE image demonstrates mild left occipital lobe atrophy. *B*, Axial CBF image shows asymmetrically decreased CBF in the left occipital lobe (*white arrows*), with corresponding decreased avidity on the axial FDG-PET image (*C*).

subsequent ASL-MR demonstrated asymmetrically decreased left temporoparietal CBF (Fig 2 and Online Supplemental Data), with confirmed β-amyloid deposition on [^{18}F] florbetaben PET and tau deposition on [^{18}F] MK-6240 PET, consistent with a diagnosis of AD (Fig 2 and Online Supplemental Data). There was also evidence of β-amyloid deposition in the parietal lobes bilaterally, but no other areas of tau deposition (Online Supplemental Data). The patient was prescribed lecanemab.

Case 3: Posterior Cortical Atrophy—the "Visual Variant" of AD

A 74-year-old woman with pre-existing hyperlipidemia, depression/anxiety, and insomnia presented with progressive forgetfulness for 2 years, as well as disorientation, worsened anxiety, and orthostasis for 4–7 years. She continued to work full-time. Examination revealed a MoCA score of 28/30, abnormal findings on bilateral Humphrey visual field testing, a left parietal drift, proprioceptive deficit and paratonia, and postural instability. MR imaging showed subtle left occipital lobe atrophy, with associated decreased CBF (Fig 3 and Online Supplemental Data). FDG-PET demonstrated corresponding decreased avidity, compatible with posterior cortical atrophy (PCA) (Fig 3 and Online Supplemental Data). The patient is considering lecanemab.

Case 4: Early-Onset PCA

A 55-year-old man with a history of hypertension and prior alcoholism, complicated by an episode of withdrawal seizures, presented with 1 year of "long COVID brain fog." The onset of symptoms was subacute after mild COVID-19 infection. Deficits included worsening dysgraphia, spatial disorientation, visual scanning deficit, simultagnosia, finger agnosia, apraxia, short-term memory lapses, and depression/anxiety, all causing disability; ADLs were preserved. His MoCA score was 7/30, complicated by severe test anxiety. CSF was borderline for AD (amyloid β 42 = 385 pg/mL, phosphorylated tau = 62.1 pg/mL, amyloid-to-tau index = 0.61). MR imaging showed moderate generalized atrophy, with decreased CBF corresponding to areas of cortical tau deposition on subsequent tau PET (Online Supplemental Data). Involvement of the left occipital lobe and visual symptoms were consistent with the clinical diagnosis of PCA, the visual variant of AD.

Case 5: Early-Onset Logopenic Variant Primary Progressive Aphasia, the "Language" Variant of AD

A 54-year-old woman presented with progressive short-term memory loss, word-finding difficulty, difficulty navigating streets, and trouble separating languages for the past several years. She remained working as a home nurse attendant. She had prediabetes, hyperlipidemia, and anxiety on sertraline. Her mother and maternal aunt had dementia in their 60s. She had occasional orientation deficits but full ADLs, a MoCA score of 15/30, trouble understanding complex commands, bradyphrenia, mild paratonia, and mild optic ataxia. Findings of a genetic dementia panel were negative. ASL-MR demonstrated decreased bilateral parietal and left temporal CBF (Online Supplemental Data), correlating to areas of decreased FDG-PET avidity, compatible with logopenic variant progressive aphasia (lvPPA) (Online Supplemental Data). This patient is a lecanemab candidate and is awaiting insurance coverage for an amyloid PET scan.

Case 6: lvPPA

A 76-year-old man presented with a progressive expressive language deficit, short-term memory loss, visual scanning difficulty, executive dysfunction, and difficulty with higher-level thinking for 4 years. He had hypertension, hyperlipidemia, and 2 maternal aunts with dementia in their 80s. He required reminders for some ADLs but could still follow current events. While his MoCA score was 4/30, he expressed complex concepts despite bradyphrenia, read with some hesitation, wrote, and repeated back risks of therapies. He had a mild postural tremor and ataxic gait. ASL-MR demonstrated decreased bilateral parietal, left-frontal and left-temporal CBF (Online Supplemental Data), more pronounced in extent than the degree of hypometabolism on FDG-PET (Online Supplemental Data). The asymmetric pattern and language deficit were compatible with lvPPA. Amyloid PET revealed diffuse cortical amyloid deposition (Online Supplemental Data).

Case 7: Progressive Supranuclear Palsy

A 59-year-old woman presented with progressive speech difficulty, short-term memory loss, apraxia, anxiety, and falls, progressing for 3 years and now needing reminders for ADLs. Her MoCA score was 15/30; she had prominent perseveration, dysarthria, phonemic paraphasia, terseness, and Parkinsonism with limited upgaze and postural instability. CSF protein and myelic basic protein were slightly elevated. MR imaging showed midbrain atrophy, suggestive of the "hummingbird" sign of progressive supranuclear palsy. This diagnosis was supported by decreased CBF and FDG avidity in the frontal lobes and [^{123}I] loflupane SPECT (DaTscan; GE Healthcare) findings indicating reduced radiotracer activity in the left caudate and left putamina greater than the right (Online Supplemental Data).

DISCUSSION

Our case series, which includes early and late onset of amnestic, visual, and language variants of AD and atypical parkinsonism, illustrates the clinical utility of ASL-MR in the management of individual patients with MCI or mild dementia. Most of the patients presented here had only mild, nonspecific volume loss on the volumetric T1-weighted sequence. However, ASL-MR was abnormal in all patients, with specific areas of decreased CBF corresponding to hypometabolism (cases 1, 3, 5, 6, and 7) or amyloid and tau deposition (cases 1, 2, 4, and 6) on PET. These findings lend strong support for an add-on, 4.5-minute, clinical noncontrast ASL-MR image to increase the sensitivity and utility of a routine clinical standard-of-care MR imaging for cognitive impairment.

The utility of ASL-MR as a proxy for FDG-PET in neurodegenerative disease has previously been described primarily in research settings. The concept that decreased CBF should approximate hypometabolism on FDG-PET arose from the observation that perfusion and metabolism in the brain are tightly coupled.[5] Indeed, studies in patients with AD that used both ASL-MR and FDG-PET found a high degree of overlap between the abnormalities found on the 2 modalities.[4,6] Additionally, studies in small AD cohorts have reported similar diagnostic accuracies between ASL-MR and FDG-PET.[7,8] However, ASL-MR is still not yet widely used in the clinical realm for this indication. One reason may be that MR imaging in neurodegenerative disease has traditionally been used largely to exclude treatable causes of dementia, because the sensitivity and specificity of structural MR imaging alone for diagnosing AD is modest and no previous disease-modifying AD treatments existed. Furthermore, ASL-MR relies on arterial blood water as an endogenous tracer, which results in a low SNR, initially limiting radiologists' confidence. However, image quality has improved substantially, supporting the clinical use, as shown in our case series.

An added novelty of our case series compared with the existing literature is that we included atypical variants of neurodegenerative disease. Thus, we demonstrate the diagnostic utility of different patterns of decreased CBF and their correlation with subsequent PET findings to illustrate the clinical utility of ASL-MR beyond the typical Alzheimer pattern. Our findings are concordant with the previously demonstrated advantage of ASL-MR in its ability to identify hypoperfusion before substantial volume loss, often exhibiting greater degrees of CBF reductions than grey matter tissue loss in affected regions (Online Supplemental Data).[9] In some cases, CBF changes were more pronounced than their subtle FDG-PET hypometabolic correlates; this finding also suggests the high sensitivity of ASL-MR. Furthermore, we provide evidence for spatial overlap of CBF abnormalities and PET amyloid and tau deposition, suggesting that CBF can reflect underlying disease pathology.

The utility of FDG-PET in the diagnosis of atypical parkinsonism syndromes has been described, but ASL-MR has been described less.[10] One study described CBF differences in Parkinson disease versus Parkinson-Plus syndrome but did not differentiate among the Parkinson-Plus syndromes.[11] Case 7 in our series exemplifies the utility of ASL-MR in identifying frontal hypoperfusion, which corresponds to FDG-PET findings of frontal hypometabolism in progressive supranuclear palsy. While the hummingbird sign on structural MR imaging is specific for a diagnosis of progressive supranuclear palsy, frontal hypometabolism seen on FDG-PET has been shown to correlate with disease duration and cognition, adding prognostic value beyond structural MR imaging.[12]

In summary, our case series is a small representation of our growing patient cohort that has received a standardized, clinical MR imaging protocol including ASL-MR and has demonstrated a spectrum of clinical severity of underlying Alzheimer disease and other neurodegenerative pathologies, from subjective impairment to MCI to dementia. We have found that ASL-MR is a highly sensitive screening tool for these pathologies. We have used CBF abnormalities to guide us toward further work-up, either via FDG-PET, amyloid/tau PET, and/or CSF sampling. In our case series, there was limited cerebrovascular burden (Online Supplementary Data), but future work can consider the impact of comorbid severe vascular disease on CBF.[13] Additionally, CBF is only a surrogate measure of neuronal activity based on neurovascular coupling,[14] so future work will evaluate instances of discordance between CBF and FDG and underlying pathophysiologic mechanisms for this discordance. Nevertheless, incorporation of this cost-effective technology into cognitive screening in the primary care or neurology clinical setting could translate into a profound population health impact, especially at a time when disease-modifying treatment is available, including the antiamyloid monoclonal antibody therapies, such as lecanemab.[15,16] These interventions are possibly most effective when initiated early, even presymptomatically, strengthening our case for the need to identify effective screening modalities.[16]

CONCLUSIONS

Our case series is concordant with prior knowledge that functional changes typically precede structural changes in patients with neurodegenerative disease. In each case of neurodegenerative disease presented, ASL-MR was an appropriate proxy for FDG-PET findings and, in some cases, amyloid and tau deposition. These patients are a small sample of our larger cohort of patients with CBF correlates to neurodegenerative disease with a wide spectrum of presentations. With standardization in clinical practice and technologic advancements in ASL-MR, CBF has

become a useful screening tool. Further investigations are necessary to support the widespread systematic deployment of this efficient and cost-effective cognitive screening tool in the race to identify, treat, and perhaps even monitor longitudinal change and treatment response in neurodegenerative disease from its earliest stages.

Disclosure forms provided by the authors are available with the full text and PDF of this article at www.ajnr.org.

REFERENCES

1. Bloudek LM, Spackman DE, Blankenburg M, et al. **Review and meta-analysis of biomarkers and diagnostic imaging in Alzheimer's disease**. *J Alzheimers Dis* 2011;26:627–45 CrossRef Medline
2. **CMS expands access to beta amyloid PET for medicare beneficiaries.** https://www.acr.org/Advocacy-and-Economics/Advocacy-News/Advocacy-News-Issues/In-the-Oct-14-2023-Issue/CMS-Expands-Access-to-Beta-Amyloid-PET-for-Medicare-Beneficiaries#:~:text=CMS%20Expands%20Access%20to%20Beta%20Amyloid%20PET%20for%20Medicare%20Beneficiaries,-Share&text=The%20Centers%20for%20Medicare%20and,(PET)%20dementia%20care%20use
3. Wolk DA, Detre JA. **Arterial spin labeling MRI: an emerging biomarker for Alzheimer's disease and other neurodegenerative conditions**. *Curr Opin Neurol* 2012;25:421–28 CrossRef Medline
4. Riederer I, Bohn KP, Preibisch C, et al. **Alzheimer disease and mild cognitive impairment: integrated pulsed arterial spin-labeling MRI and 18F-FDG PET.** *Radiology* 2018;288:198–206 CrossRef Medline
5. Buxton RB, Frank LR. **A model for the coupling between cerebral blood flow and oxygen metabolism during neural stimulation.** *J Cereb Blood Flow Metab* 1997;17:64–72 CrossRef Medline
6. Chen Y, Wolk DA, Reddin JS, et al. **Voxel-level comparison of arterial spin-labeled perfusion MRI and FDG-PET in Alzheimer disease.** *Neurology* 2011;77:1977–85 CrossRef Medline
7. Musiek ES, Chen Y, Korczykowski M, et al. **Direct comparison of fluorodeoxyglucose positron emission tomography and arterial spin labeling magnetic resonance imaging in Alzheimer's disease**. *Alzheimers Dement* 2012;8:51–59 CrossRef Medline
8. Ceccarini J, Bourgeois S, Van Weehaeghe D, et al. **Direct prospective comparison of 18F-FDG PET and arterial spin labelling MR using simultaneous PET/MR in patients referred for diagnosis of dementia.** *Eur J Nucl Med Mol Imaging* 2020;47:2142–54 CrossRef Medline
9. Johnson NA, Jahng GH, Weiner MW, et al. **Pattern of cerebral hypoperfusion in Alzheimer disease and mild cognitive impairment measured with arterial spin-labeling MR imaging: initial experience.** *Radiology* 2005;234:851–59 CrossRef Medline
10. Zhao P, Zhang B, Gao S. **18[F]-FDG PET study on the idiopathic Parkinson's disease from several parkinsonian-plus syndromes**. *Parkinsonism Relat Disord* 2012;18(Suppl 1):S60–22 CrossRef Medline
11. Cheng L, Wu X, Guo R, et al. **Discriminative pattern of reduced cerebral blood flow in Parkinson's disease and Parkinsonism-Plus syndrome: an ASL-MRI study**. *BMC Med Imaging* 2020;20:78 CrossRef Medline
12. Blin J, Baron JC, Dubois B, et al. **Positron emission tomography study in progressive supranuclear palsy.** *Arch Neurol* 1990;47:747–52 CrossRef Medline
13. Telischak NA, Detre JA, Zaharchuk G. **Arterial spin-labeling MRI: clinical applications in the brain.** *J Magn Reson Imaging* 2015;41:1165–80 CrossRef Medline
14. Zhu WM, Neuhaus A, Beard DJ, et al. **Neurovascular coupling mechanisms in health and neurovascular uncoupling in Alzheimer's disease**. *Brain* 2022;145:2276–92 CrossRef Medline
15. van Dyck CH, Swanson CJ, Aisen P, et al. **Lecanemab in early Alzheimer's disease**. *N Engl J Med* 2023;388:9–21 CrossRef Medline
16. Sims JR, Zimmer JA, Evans CD, et al. TRAILBLAZER-ALZ 2 Investigators. **Donanemab in early symptomatic Alzheimer disease.** *JAMA* 2023;330:512–27 CrossRef Medline

Supplementary Methods:

ASL-MR sequence:

All patients were imaged on the same clinical 3 Tesla GE SIGNA Architect MRI scanner (GE Medical Systems, Milwaukee, WI, USA). The 3D pseudo-continuous ASL-MR product sequence had the following parameters: PLD 2025 ms, TR 4876, TE 53.6, 38 x 4 mm axial slices, FOV 24, matrix size 512; the scanning time was 4 minutes and 24 seconds. CBF maps were processed using the GE AW Server 3.2 ext 4.0, set to a range of 0-80 mL/100g/min using the rainbow color scheme. Images were visually interpreted in native space.

ASL-MR Z-score maps:

Twenty-eight patients (aged 45-88 years), who had been scanned on the same 3 Tesla GE MRI scanner, having initially presented with cognitive concerns, were used as a control cohort to construct Z-score maps. These control subjects had resulting normal MRI scans, as well as a clinical, cognitive, and laboratory workup that was not suggestive of a neurodegenerative disorder. Of note, a validated healthy comparison cohort and a standardized imaging processing pipeline for ASL-MR are not yet widely available from vendors and thus difficult to incorporate into routine clinical practice. In the literature, there is a wide range of image processing pipelines and parameters, which are largely lab-specific. Similarly, various “normal” control cohorts have been used in the literature, often including patients with headaches with variable confirmation by clinical/cognitive assessment, which limits widespread adoption of these Z-score maps.

In the Weill Cornell Brain Health Imaging Institute, we used the following image-processing pipeline. All subjects’ Freesurfer (FS) reconstructions were performed with FS version 7.10. The M0 image was coregistered to FS T1-weighted (T1w) space and the corresponding CBF map was converted to FS space using the transform matrix generated during M0 coregistration. Next, all subjects’ T1w in FS space were warped to the MNI152 template using the FSL fnirt command; the warping fields were saved and applied to the FS space CBF map. The mean and standard deviation (SD) of the CBF values in template space were computed for the 28 control subjects. Each patient’s CBF was Z-scored using the mean and SD of the control subjects. All processing was performed in FSL and MATLAB 2023a, and the final snapshots were taken from

FSLeyes by overlaying individual MNI space CBF on T1w. The 3D Z-score map was created by overlaying the CBF onto an MNI152 template for each subject using MRIcroGL. Images are shown in radiological convention.

Volumetric comparison:

FS segmentation was also used to obtain regional brain volumes in the 7 patients and the control cohort (n=28) as noted above. Frontal (including superior frontal, rostral middle frontal, caudal middle frontal gyri), parietal (posterior cingulate, precuneus, superior and inferior parietal lobules), temporal (superior, middle, inferior temporal gyri), and occipital (lateral occipital, lingual, cuneus) lobe regions were assessed, as well as hippocampal volumes. Brain regions were considered atrophic if volumes were 1.5 standard deviations below those of the control cohort.

FDG-PET Z-score maps:

FDG-PET images were post-processed using the widely clinically available syngo.via software (Siemens Healthineers, Erlangen, Germany). A control cohort of 33 individuals (aged 46-79), included in the software package, were used to generate Z-score maps of the SUV values using the MI Neurology workflow, overlaid onto MNI space.

Supplementary Data:

When comparing brain regional volumes of our 7 cases to our 28 controls:
Case 5 had regional volumes that were 1.5 standard deviations below the controls in the frontal (caudal middle frontal), parietal (inferior parietal, posterior cingulate, precuneus), temporal (superior temporal, middle temporal, inferior temporal), and occipital (cuneus, lateral occipital) lobes. Case 4 had atrophy that was 1.5 standard deviations below the controls in the caudal middle frontal region. None of the 7 cases had significant hippocampal atrophy.

Cortical gray matter CBF values of our 7 cases (units = mL/100g/min):

Case 1: 28

Case 2: 68

Case 3: 69

Case 4: 35

Case 5: 44

Case 6: 26

Case 7: 34

White matter hyperintensity burden for the 7 cases:

Case 1: Minimal (Fazekas grade 1)

Case 2: Mild (Fazekas grade 1)

Case 3: Mild (Fazekas grade 1)

Case 4: Mild (Fazekas grade 1)

Case 5: Minimal (Fazekas grade 1)

Case 6: Mild (Fazekas grade 1)

Case 7: Moderate (Fazekas grade 2)

Supplementary Figures:

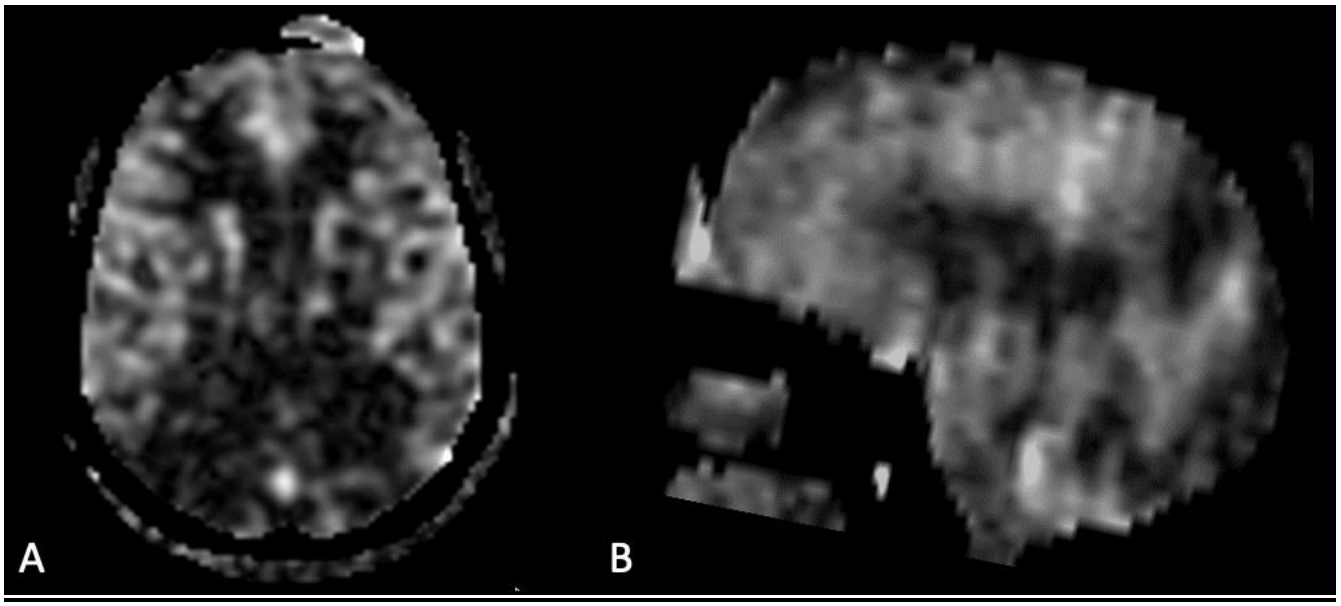

Supplementary Figure 1 (Case 1 Early-onset AD with presenilin mutation): Gray-scale axial (A) and sagittal (B) ASL-MR images showing decreased CBF in the bilateral parietal lobes, particularly on the right, and the precuneus – these are suggestive of AD.

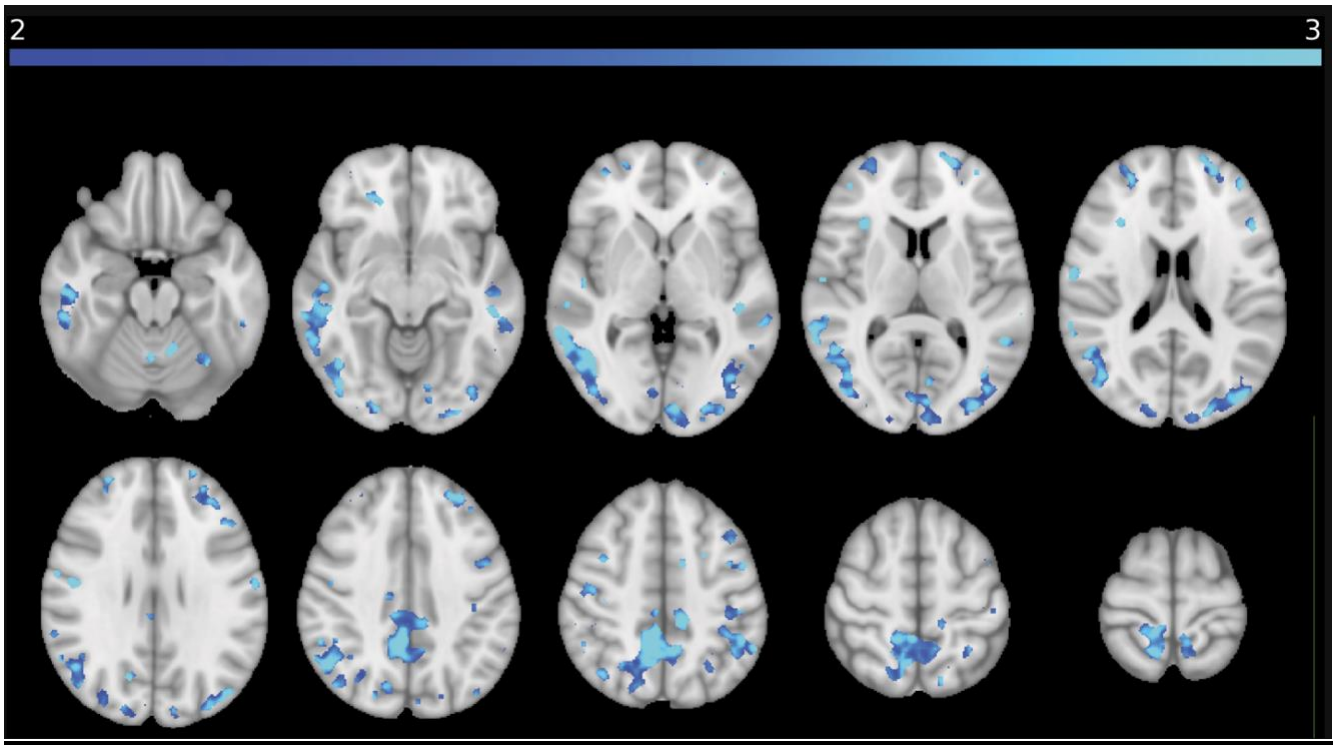

Supplementary Figure 2 (Case 1): Axial Z-score maps, with blue corresponding to areas of decreased CBF, predominantly in the temporal and parietal lobes, as compared to our control cohort. Upper and lower Z-score thresholds of 2.0 and 3.0 are shown in the color bar.

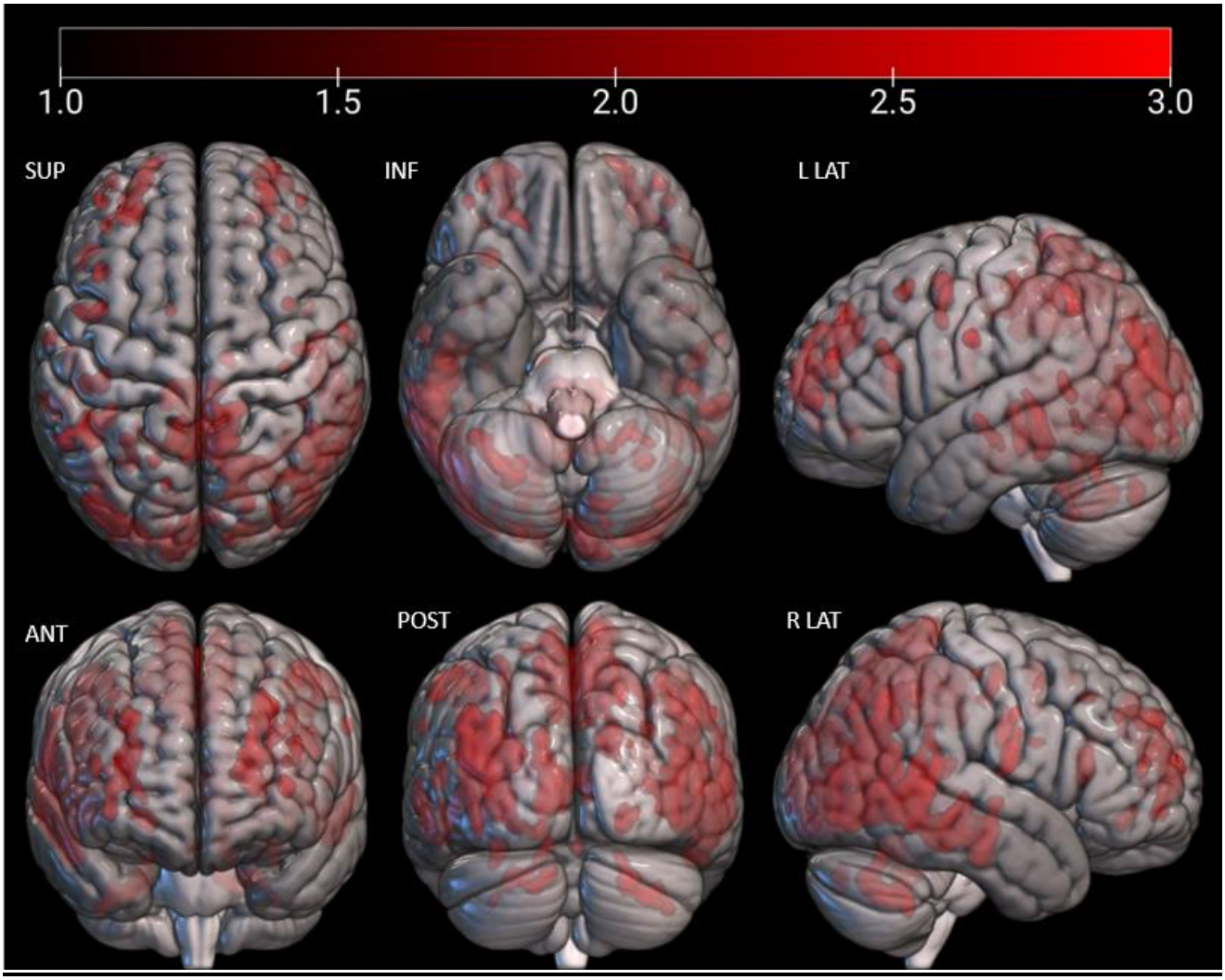

Supplementary Figure 3 (Case 1): Three-dimensional stereotactic surface projection images with red corresponding to decreased CBF, predominantly in the parietal and temporal lobes, as compared to our control cohort. Upper and lower Z-score thresholds of 1.0 and 3.0 are shown in the color bar.

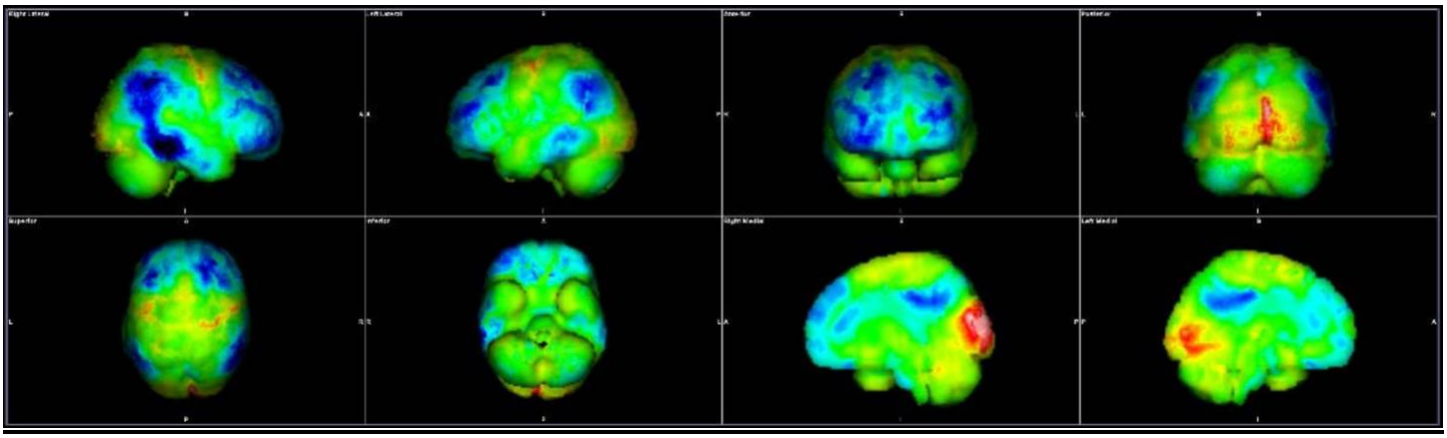

Supplementary Figure 4 (Case 1): Three-dimensional stereotactic surface projection images with blue representing the patient's decreased FDG avidity, as compared to a normative database, using the clinically available syngo.via software package.

Supplementary Figure 5 (Case 1): Axial [18F]-florbetaben PET image demonstrating diffuse cortical amyloid deposition, consistent with AD.

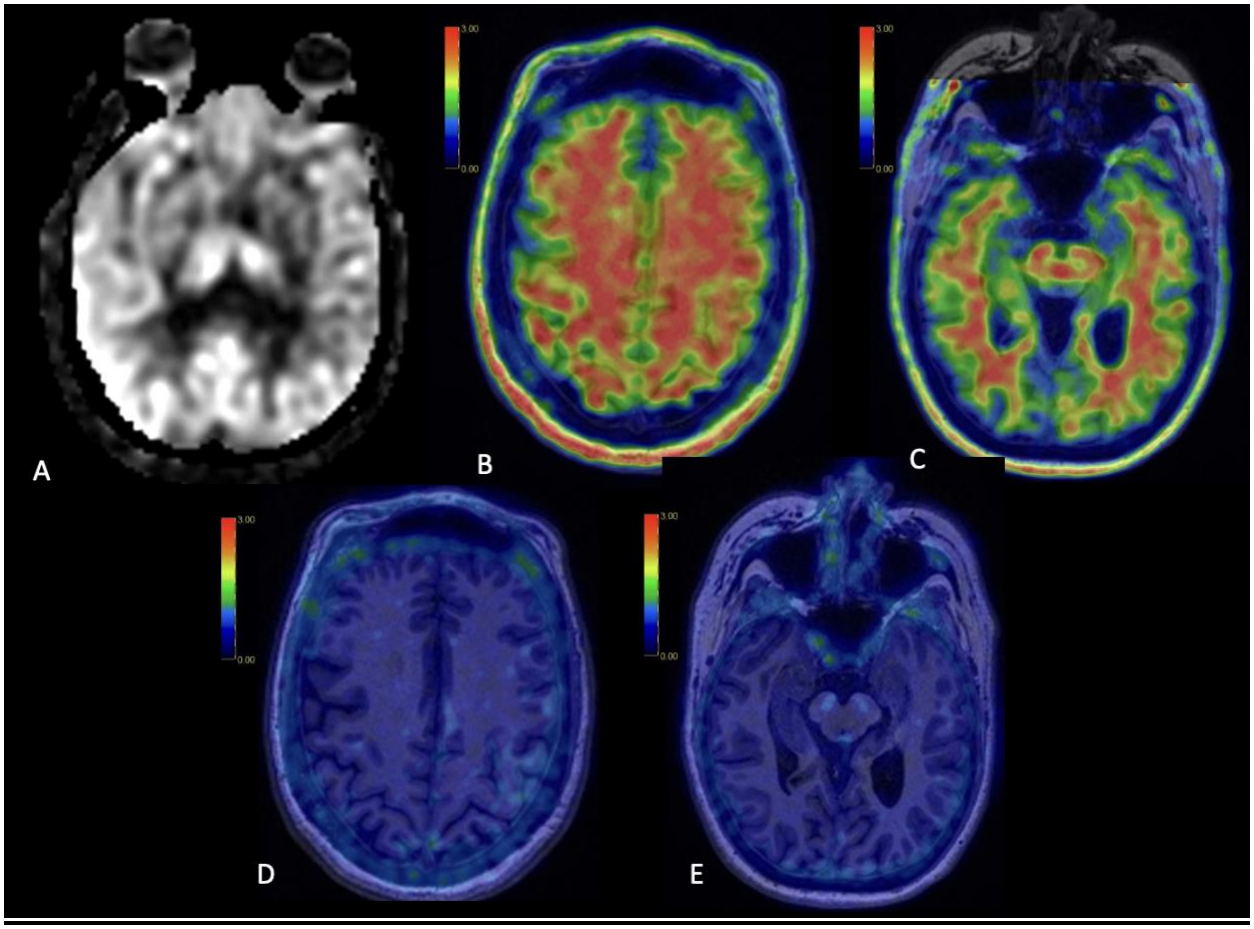

Supplementary Figure 6 (Case 2 Early-onset AD and post-COVID brain fog): Axial gray-scale ASL-MR image (A) demonstrating slightly decreased CBF at the left temporoparietal junction. Axial [18F]-florbetaben PET image (B and C) demonstrate cortical amyloid deposition in the parietal lobes and left temporal lobe. Axial [18F]-florbetaben PET images (D and E) show no evidence of cortical tau deposition in other parts of the brain.

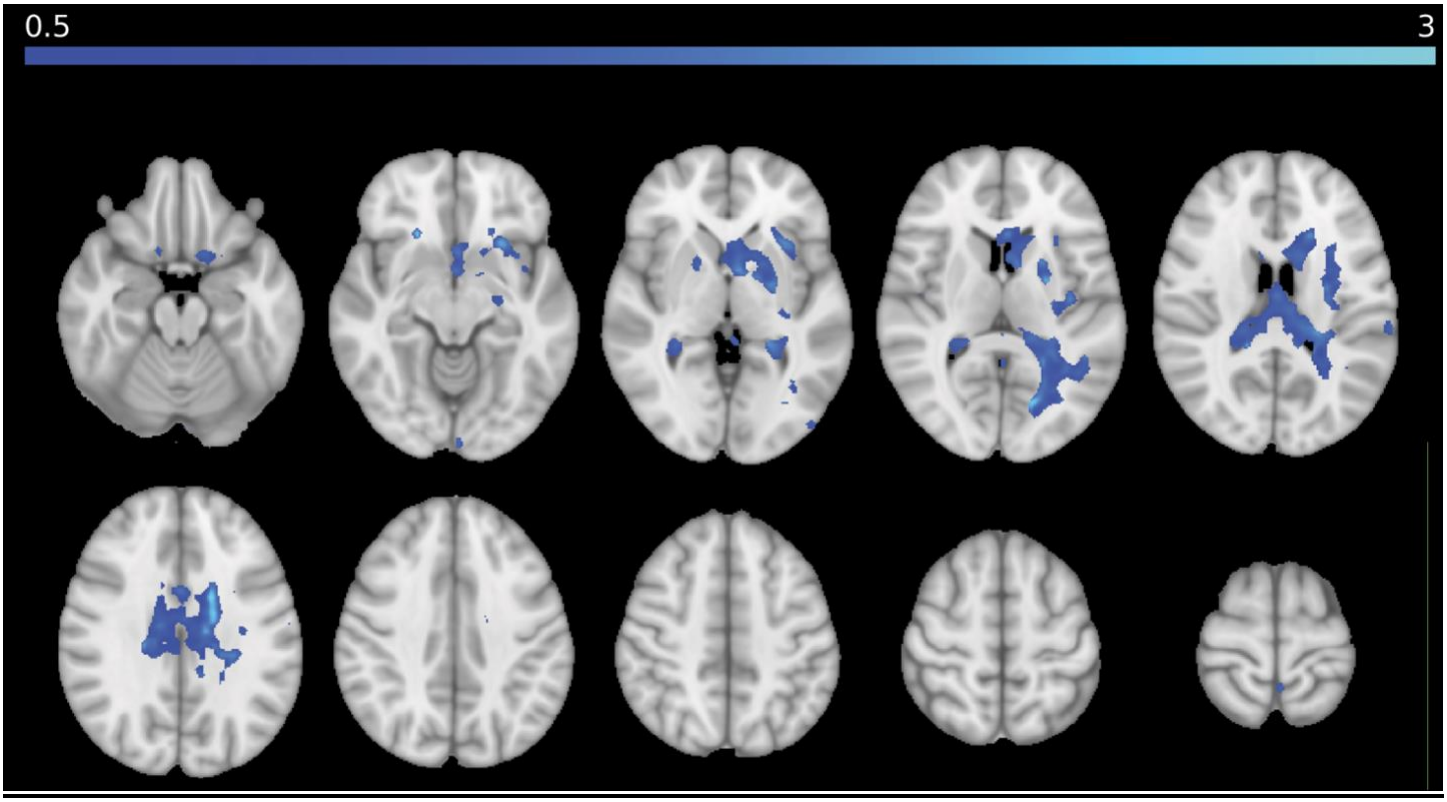

Supplementary Figure 7 (Case 2): Axial Z-score maps, with blue corresponding to areas of decreased CBF, asymmetrically involving the left temporoparietal region. Upper and lower Z-score thresholds of 0.5 and 3.0 are shown in the color bar.

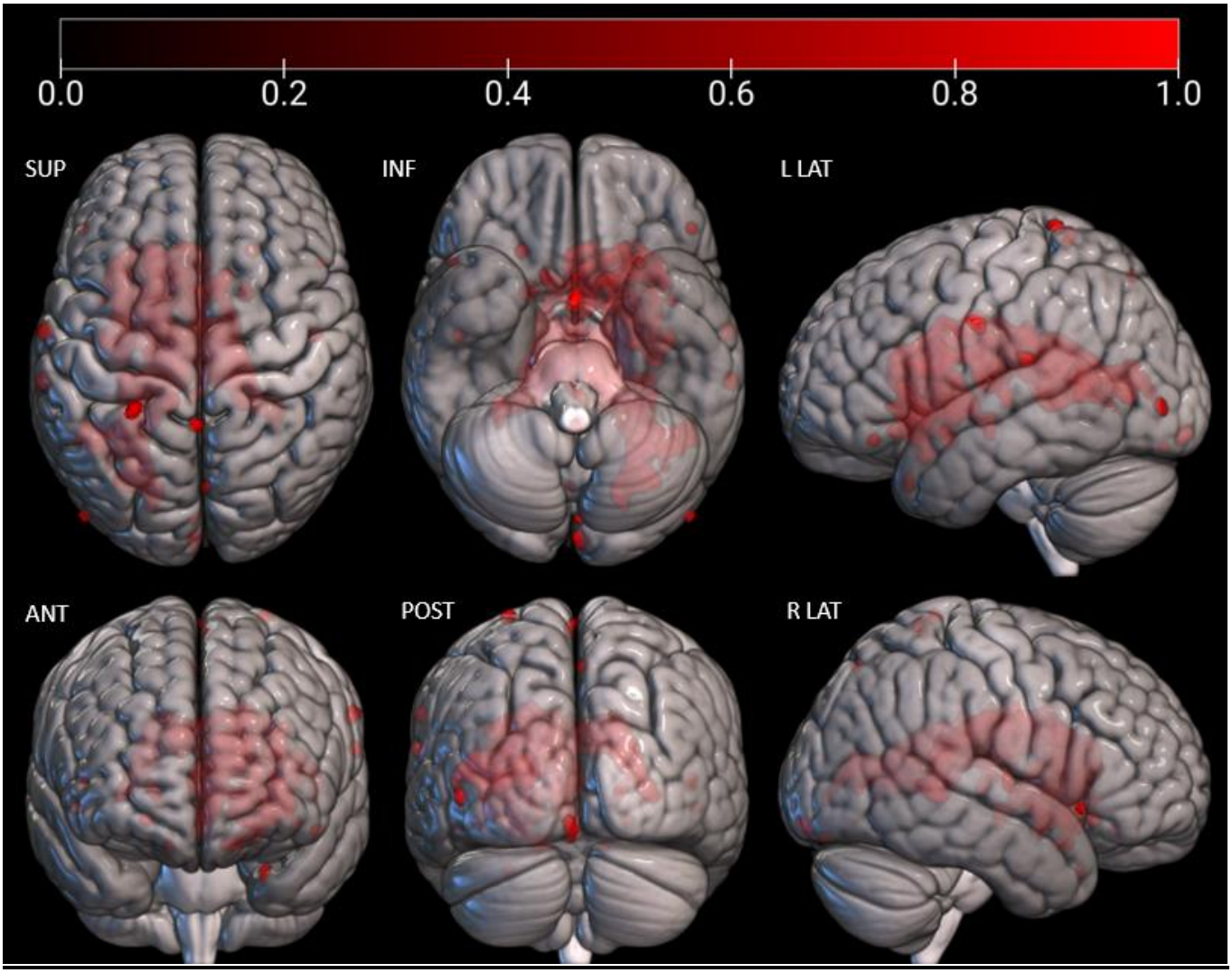

Supplementary Figure 8 (Case 2): Three-dimensional stereotactic surface projection images with red corresponding to subtle areas of decreased CBF, less clearly showing the focal area of decreased CBF in the left temporoparietal junction than on axial images. Z-score thresholds were lowered (0 and 1.0) to increase sensitivity.

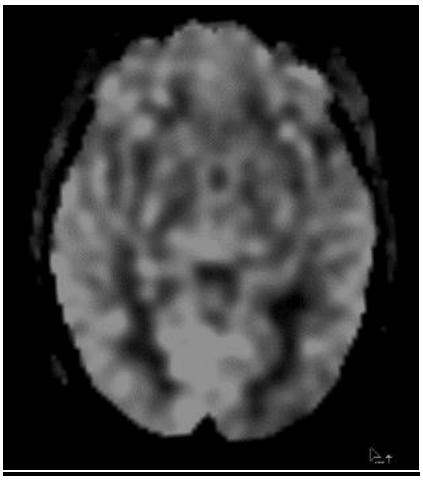

Supplementary Figure 9 (Case 3 Posterior cortical atrophy): Gray-scale axial ASL-MR image showing decreased CBF in the left occipital lobe.

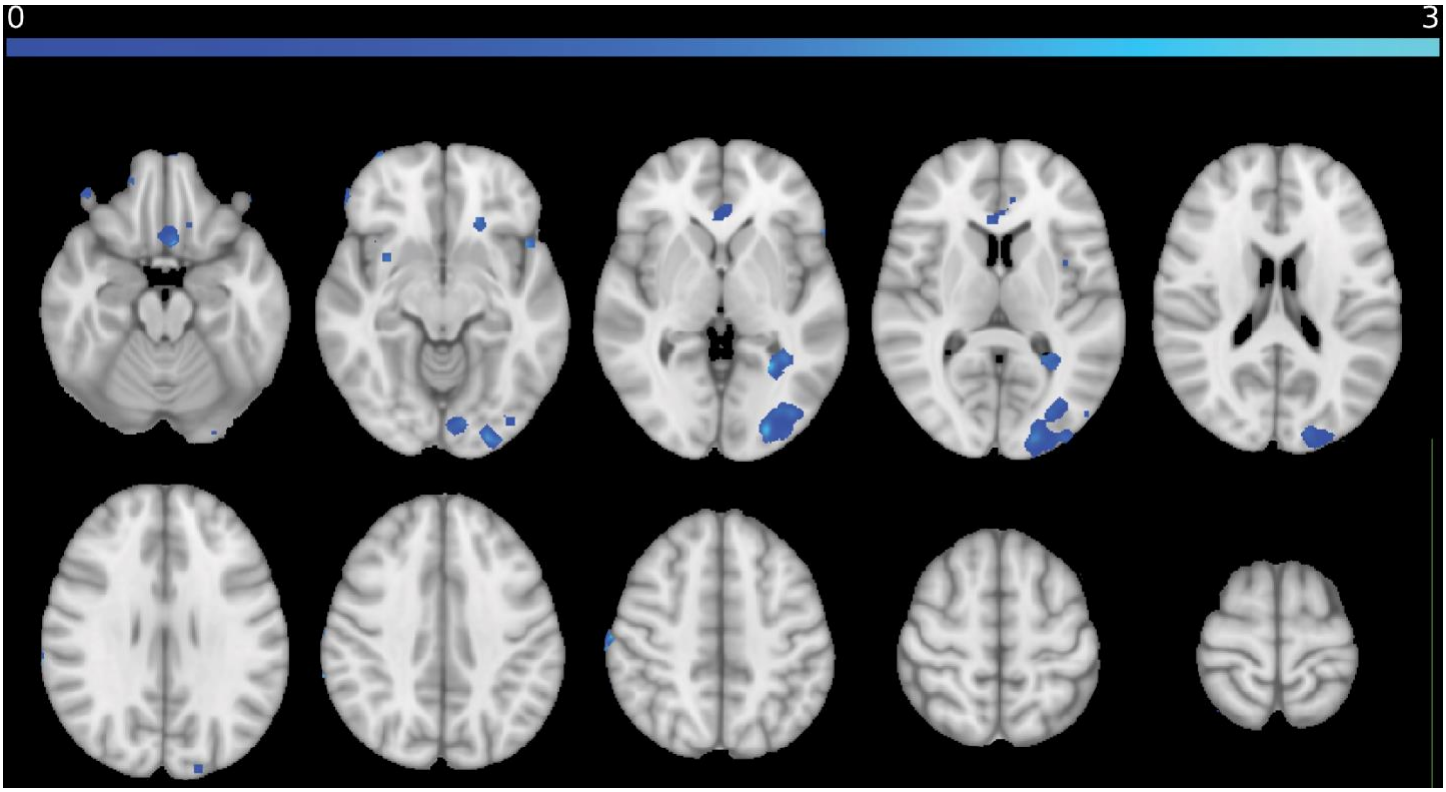

Supplementary Figure 10 (Case 3): Axial Z-score maps, with blue corresponding to areas of decreased CBF, predominantly in the left occipital lobe, as compared to our control cohort. Upper and lower Z-score thresholds of 2.0 and 3.0 were used.

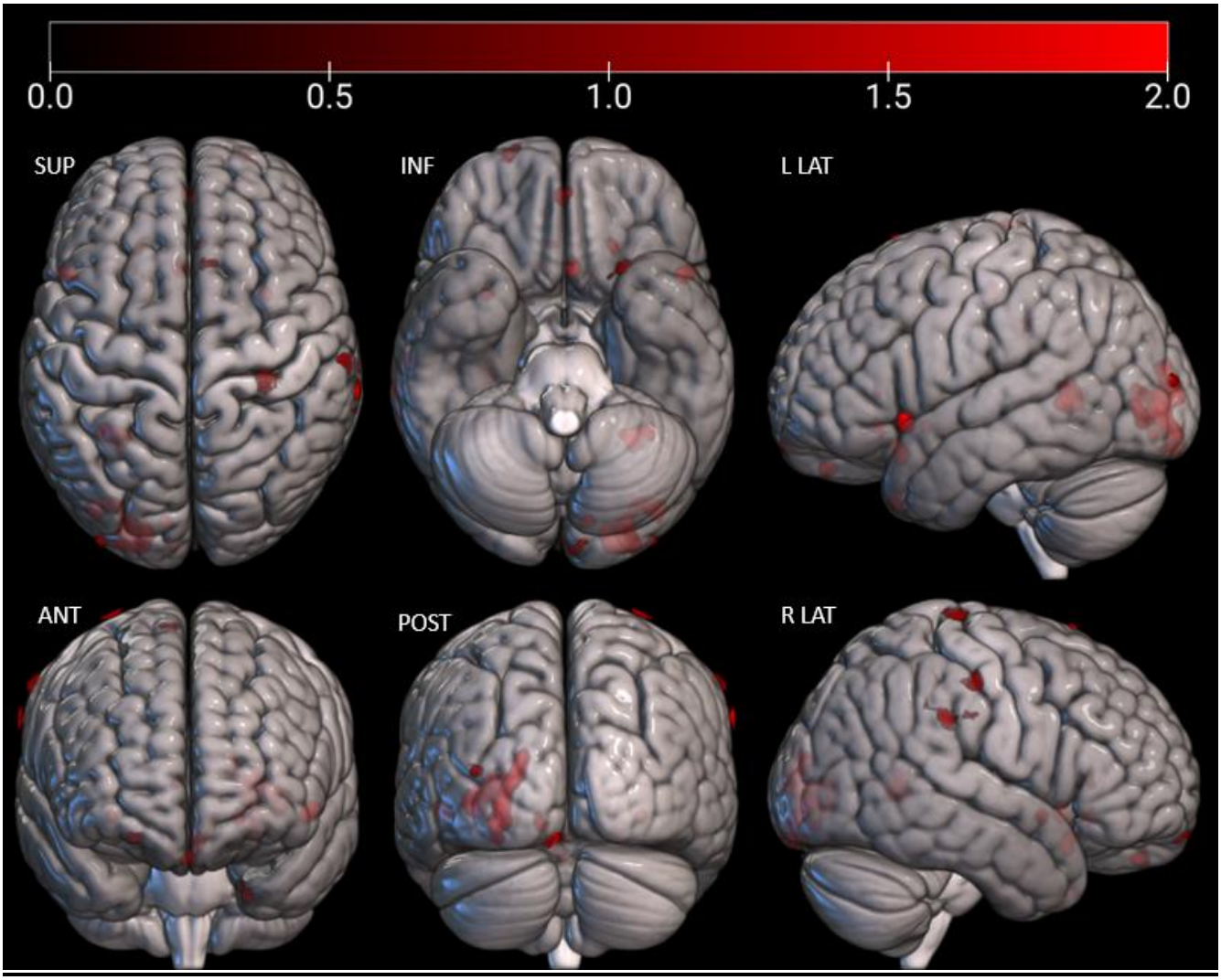

Supplementary Figure 11 (Case 3): Three-dimensional stereotactic surface projection images with red corresponding to decreased CBF, predominantly in the left occipital lobe, as compared to our control cohort. Upper and lower Z-score thresholds of 0 and 2.0 are shown in the color bar.

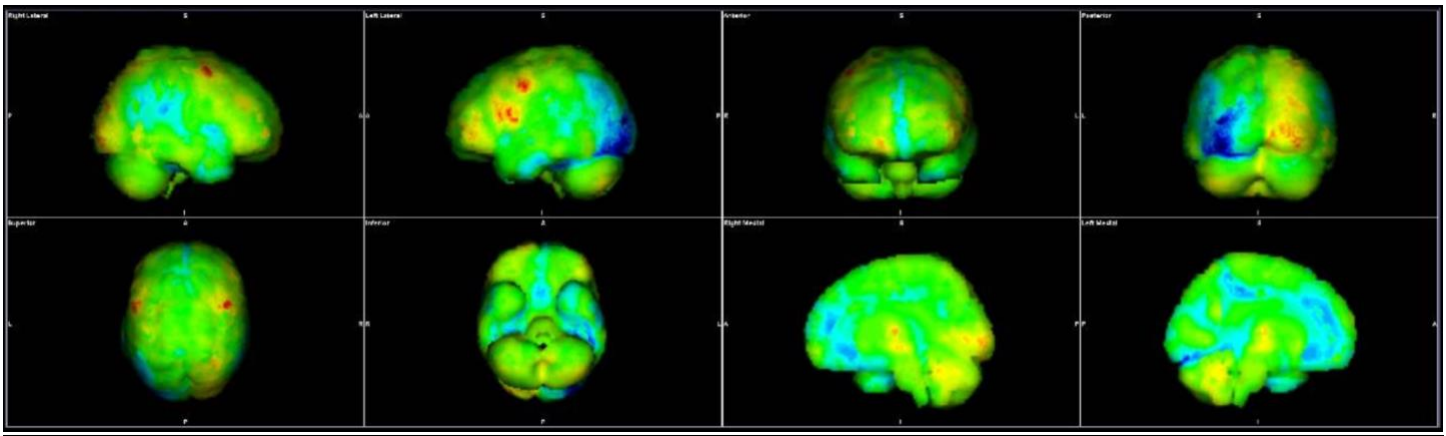

Supplementary Figure 12 (Case 3): Three-dimensional stereotactic surface projection images with blue representing the patient's decreased FDG avidity in the left occipital lobe, as compared to a normative database, using the clinically available syngo.via software package.

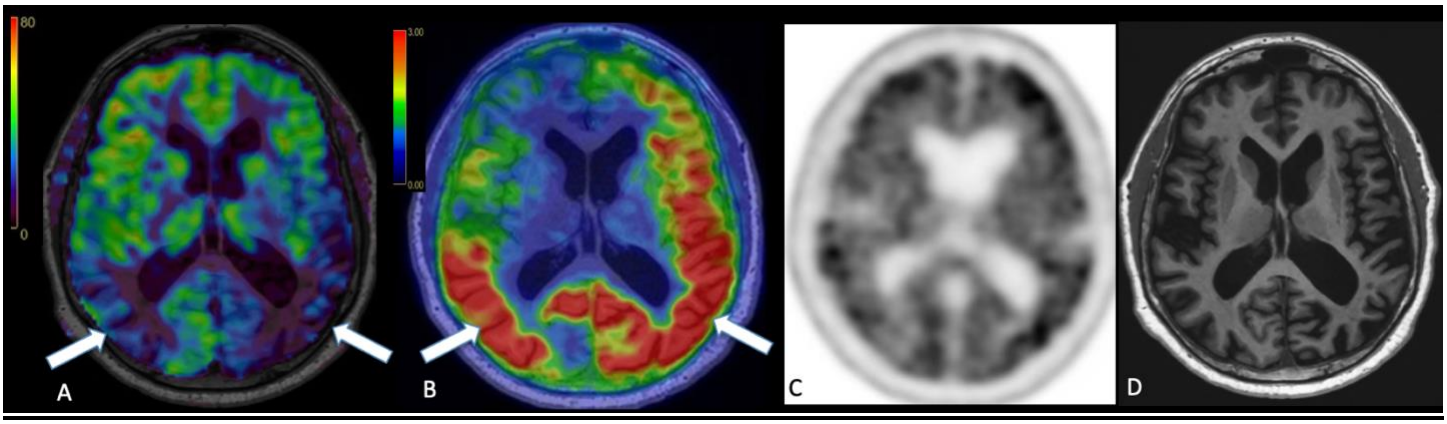

Supplementary Figure 13 (Case 4 Early-onset PCA): (A) Axial CBF image showing biparietal decreased CBF (white arrows), extending into the left occipital lobe. **(B)** Axial [18F]-MK6240 tau PET image showing cortical tau deposition corresponding to areas of decreased CBF. **(C)** Diffuse cortical amyloid deposition on the axial [11C]-Pittsburgh Compound B PET image. **(D)** Axial 3D T1 MPRAGE showing nonspecific moderate generalized atrophy.

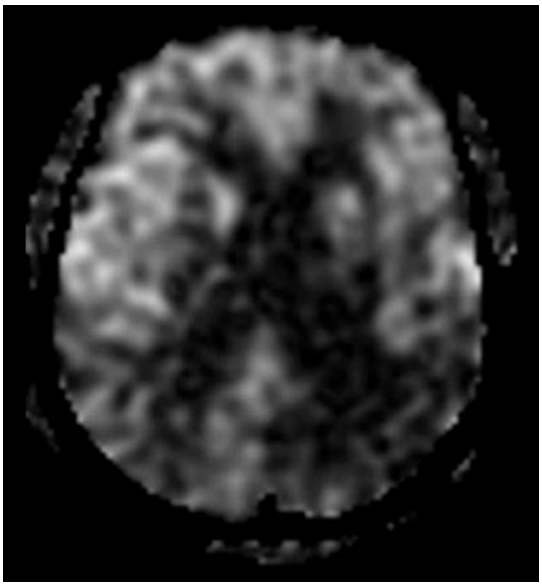

Supplementary Figure 14 (Case 4): Gray-scale axial ASL-MR image demonstrating decreased CBF in the bilateral parietal lobes, particularly on the left.

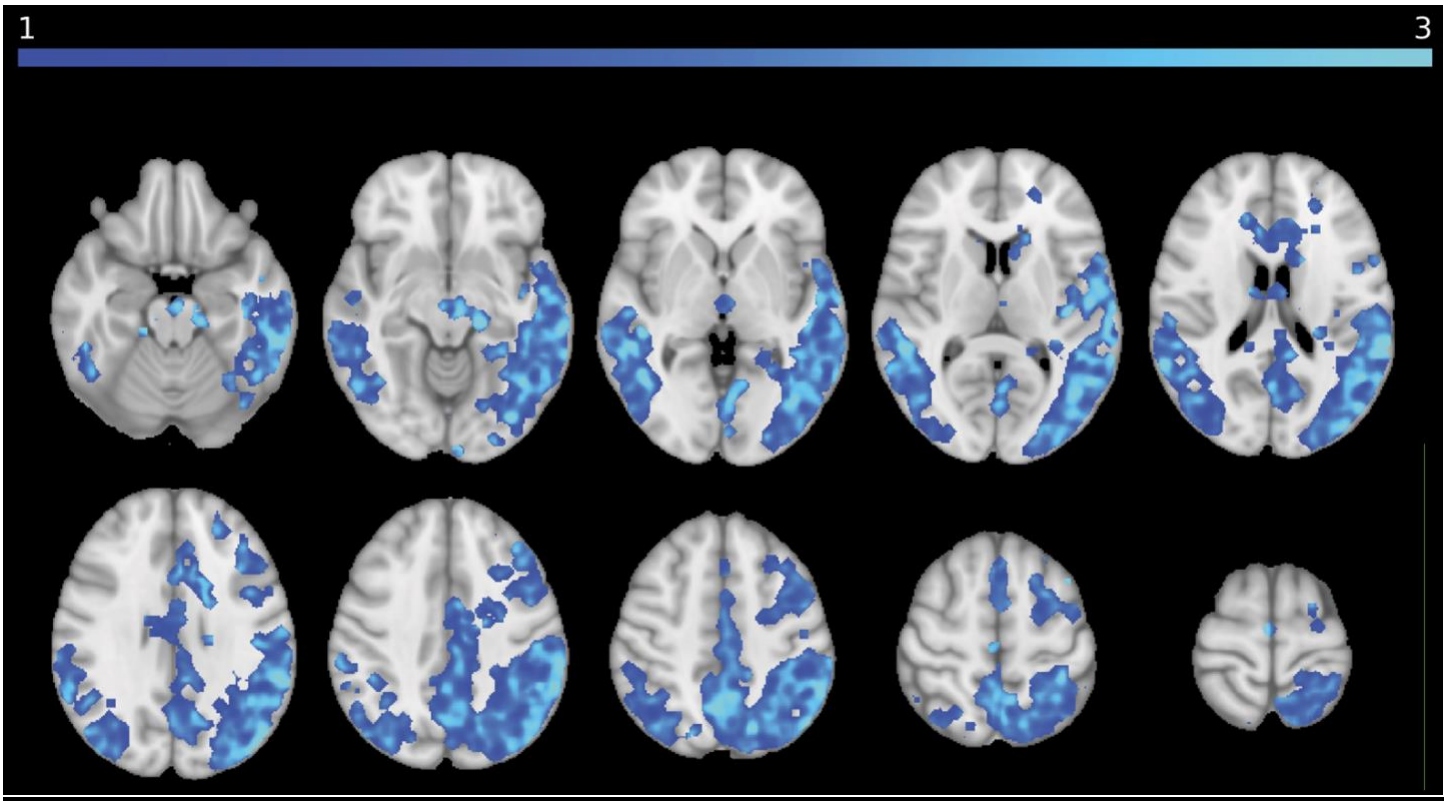

Supplementary Figure 15 (Case 4): Axial Z-score maps, with blue corresponding to areas of decreased CBF, predominantly in the temporal and parietal lobes, more pronounced on the left, as well as the left frontal lobe. Upper and lower Z-score thresholds of 1.0 and 3.0 are shown in the color bar.

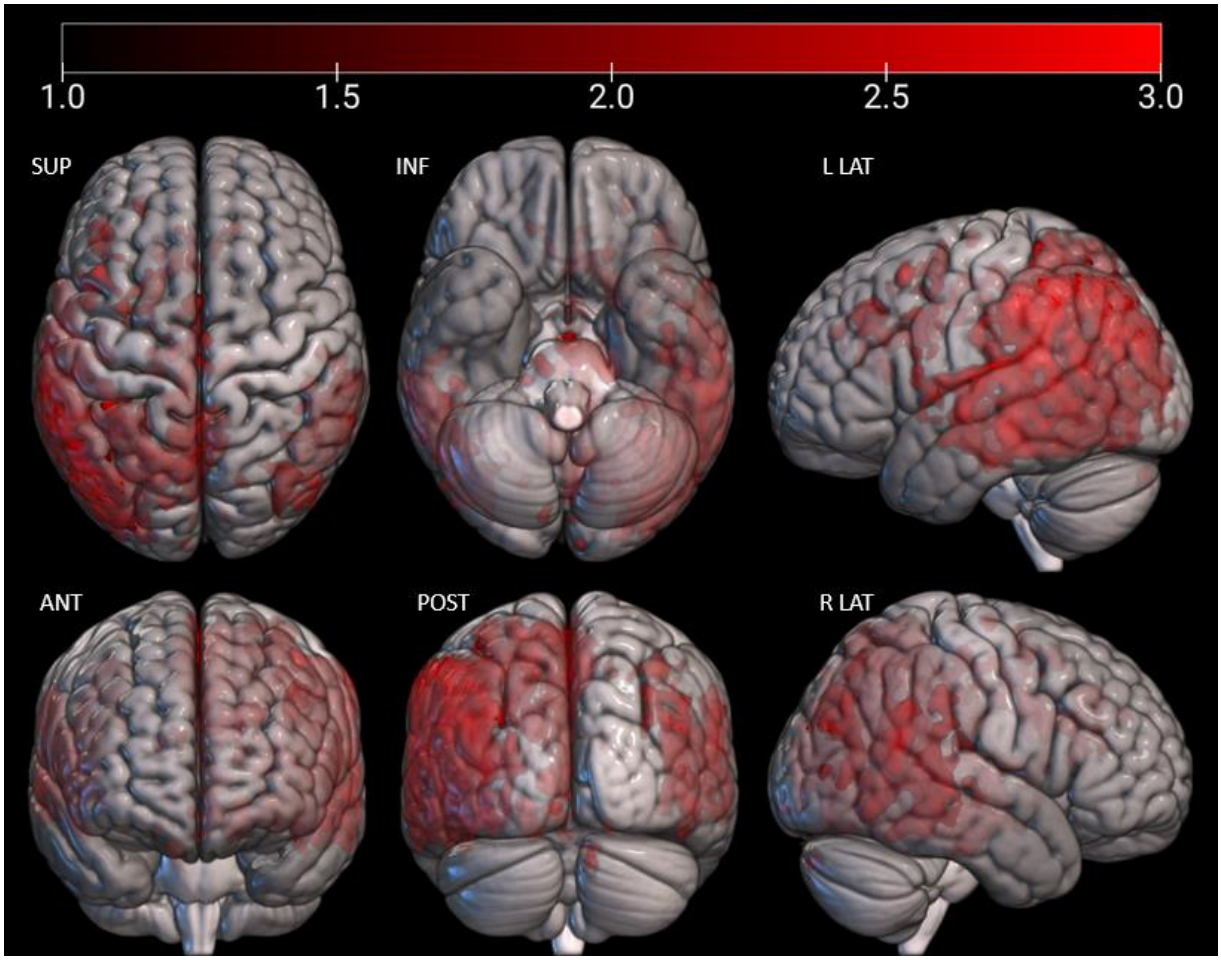

Supplementary Figure 16 (Case 4): Three-dimensional stereotactic surface projection images with red corresponding to decreased CBF, predominantly in the parietal and temporal lobes, as well as the left frontal lobe. Upper and lower Z-score thresholds of 1.0 and 3.0 are shown in the color bar.

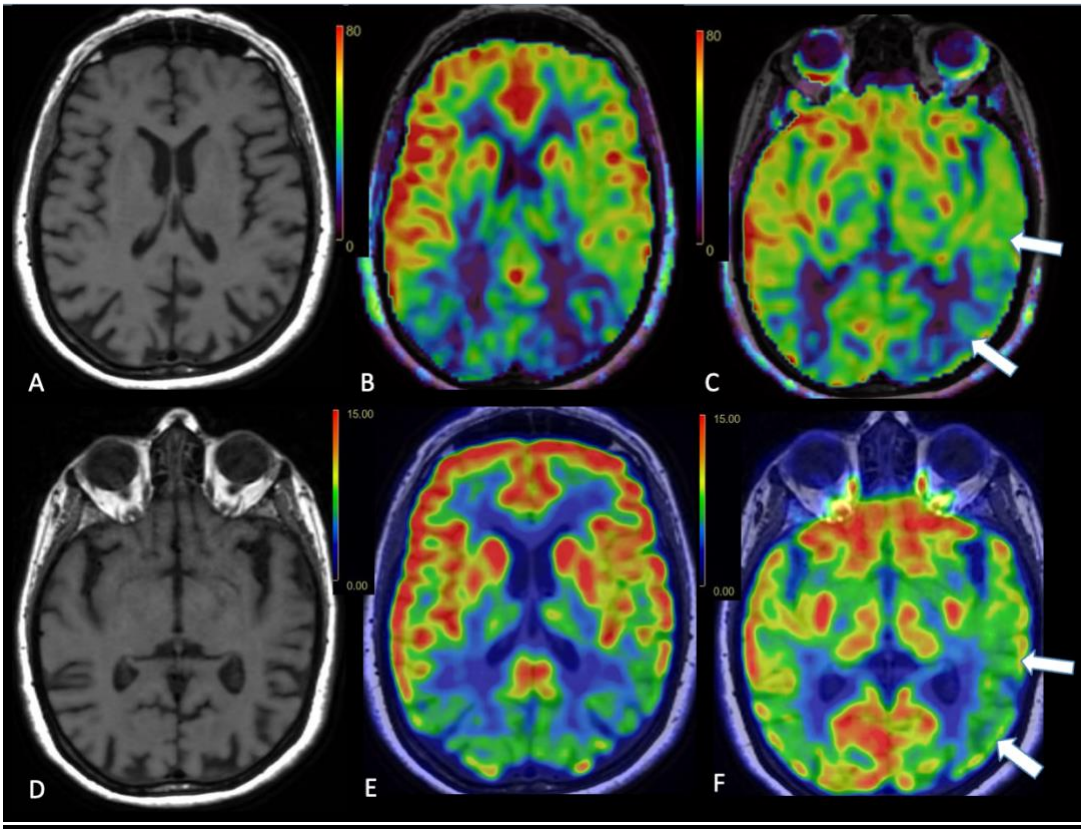

Supplementary Figure 17 (Case 5 Early-onset lvPPA AD): MR was notable for mild generalized volume loss with subtle asymmetric dilation of the left ventricular atrium **(A,D)**. ASL-MR showing decreased CBF in the bilateral parietal lobes **(B)**, also involving the left temporal lobe asymmetrically **(C) (white arrows)**, corresponding to decreased cortical FDG avidity on PET **(E,F)**.

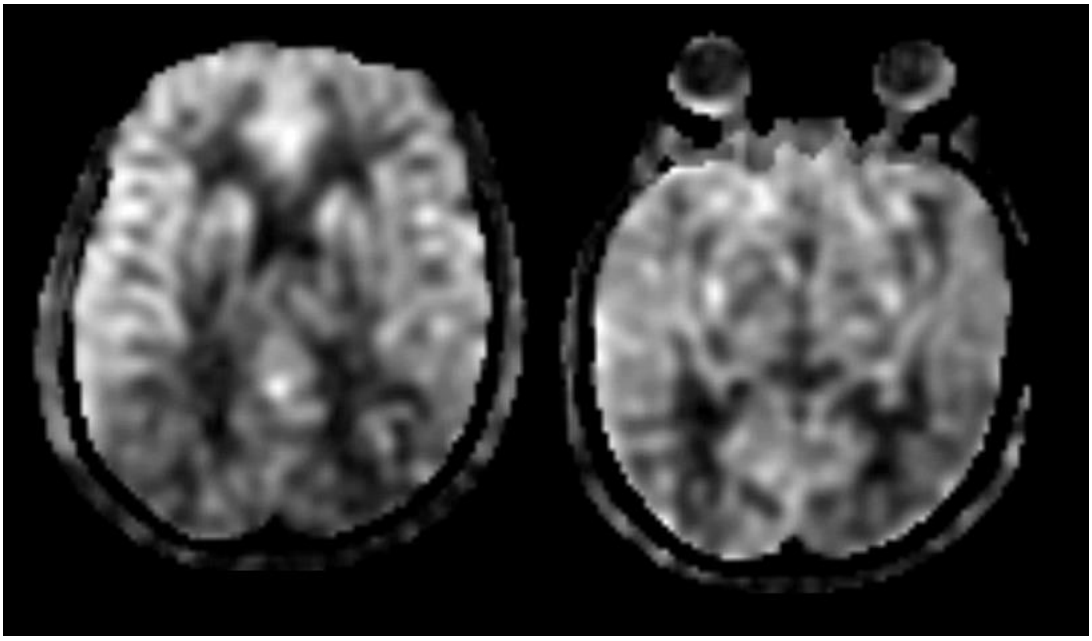

Supplementary Figure 18 (Case 5): Gray-scale axial ASL-MR images demonstrating decreased CBF in the bilateral parietal and left temporal lobes, suggestive of neurodegenerative disease.

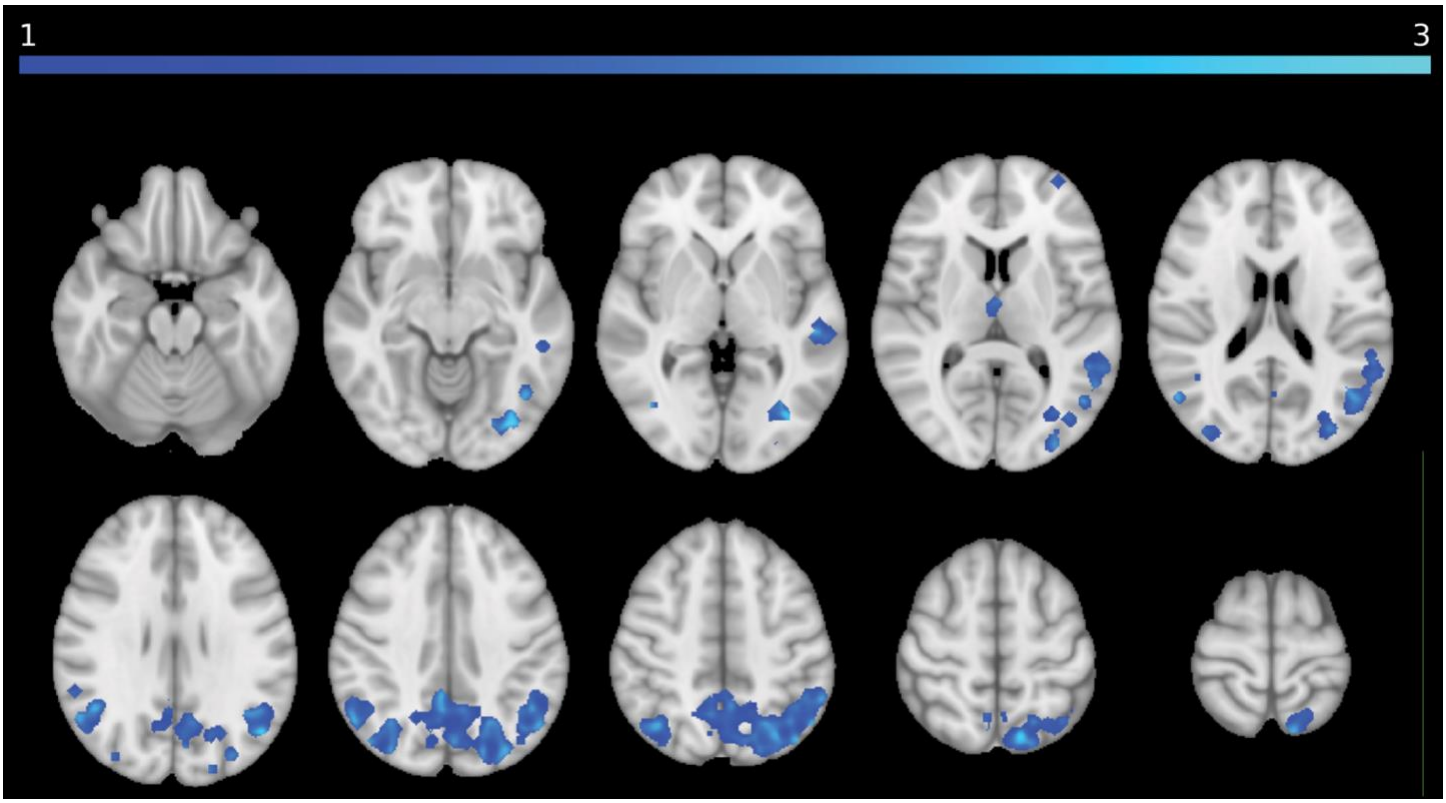

Supplementary Figure 19 (Case 5): Axial Z-score maps, with blue corresponding to areas of decreased CBF in the bilateral parietal and left temporal lobes, as compared to our control cohort. Upper and lower Z-score thresholds of 1.0 and 3.0 are shown in the color bar.

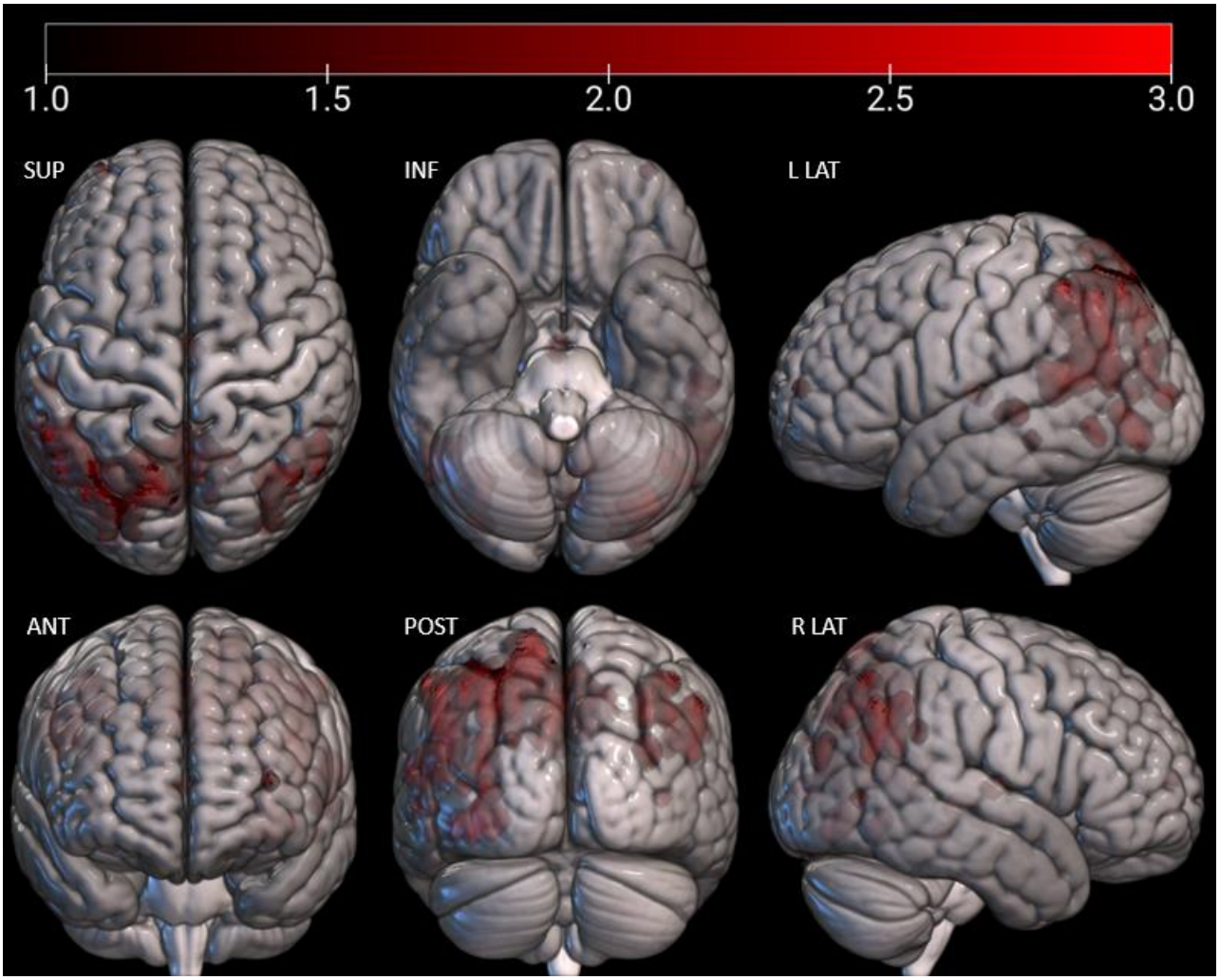

Supplementary Figure 20 (Case 5): Three-dimensional stereotactic surface projection images with red corresponding to decreased CBF in the bilateral parietal and left temporal lobes, as compared to our control cohort. Upper and lower Z-score thresholds of 1.0 and 3.0 are shown in the color bar.

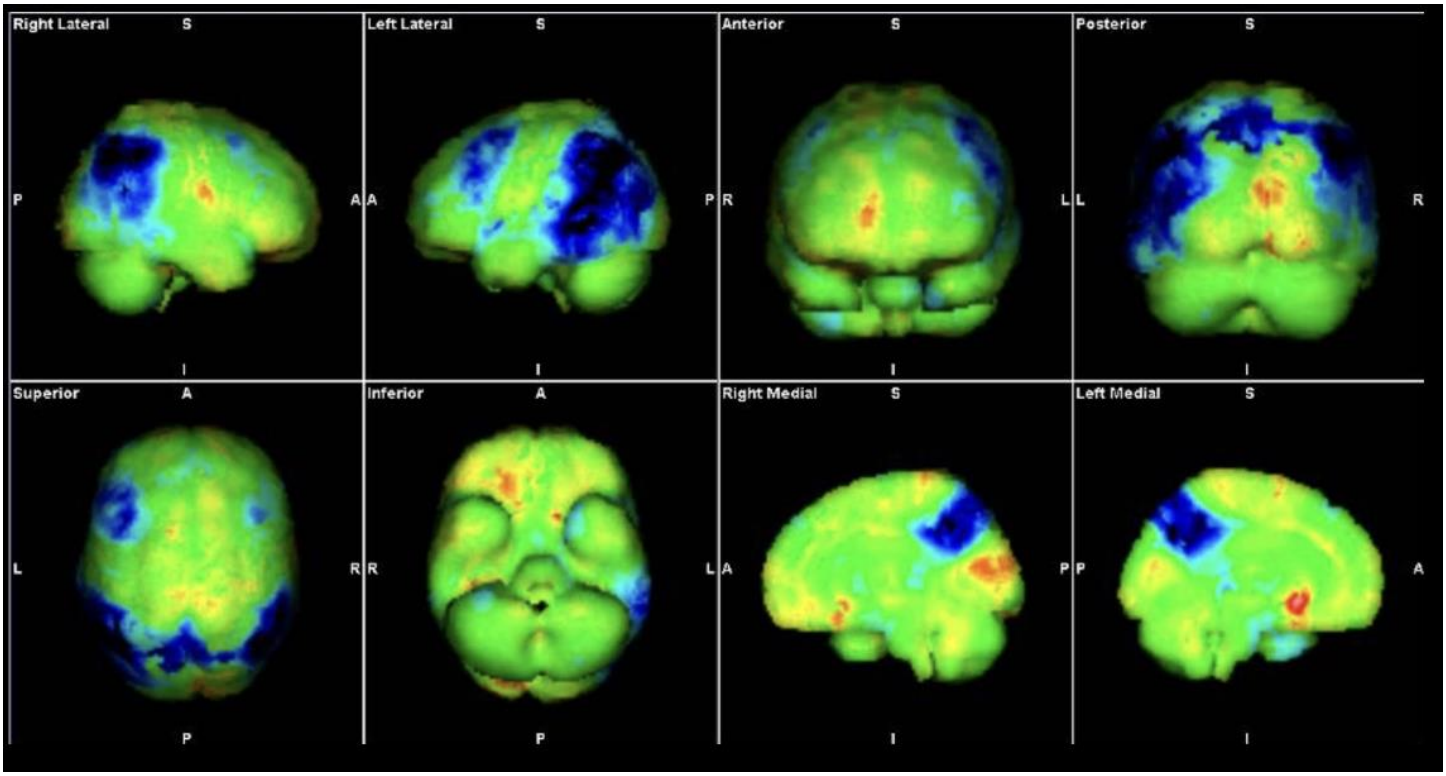

Supplementary Figure 21 (Case 5): Three-dimensional stereotactic surface projection images with blue representing the patient's decreased FDG avidity in the bilateral parietal and temporal lobes, as well as the precuneus bilaterally and left frontal lobe.

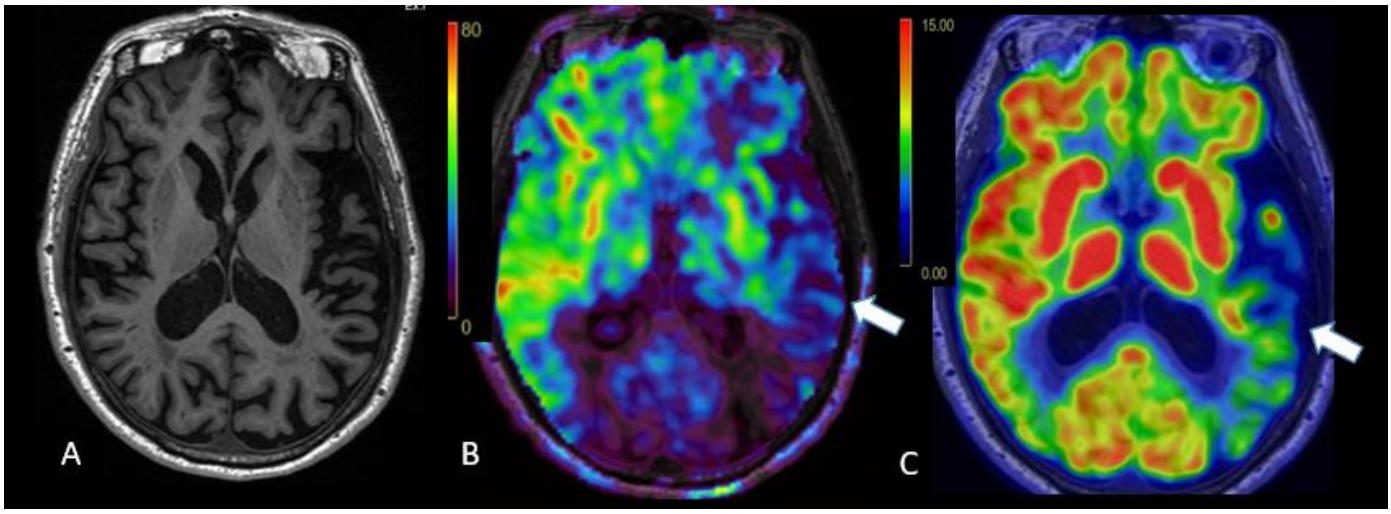

Supplementary Figure 22 (Case 6 lvPPA). (A) Axial 3D T1 MPRAGE image demonstrating moderate generalized volume loss. **(B)** Axial ASL-MR image showing decreased CBF in the bilateral parietal lobes, more pronounced on the left, as well as the left frontal and temporal lobes. **(C)** Axial FDG-PET image showing decreased FDG avidity in the left parietal (white arrow) and temporal lobes, as well as the right parietal and left frontal lobes to a lesser extent.

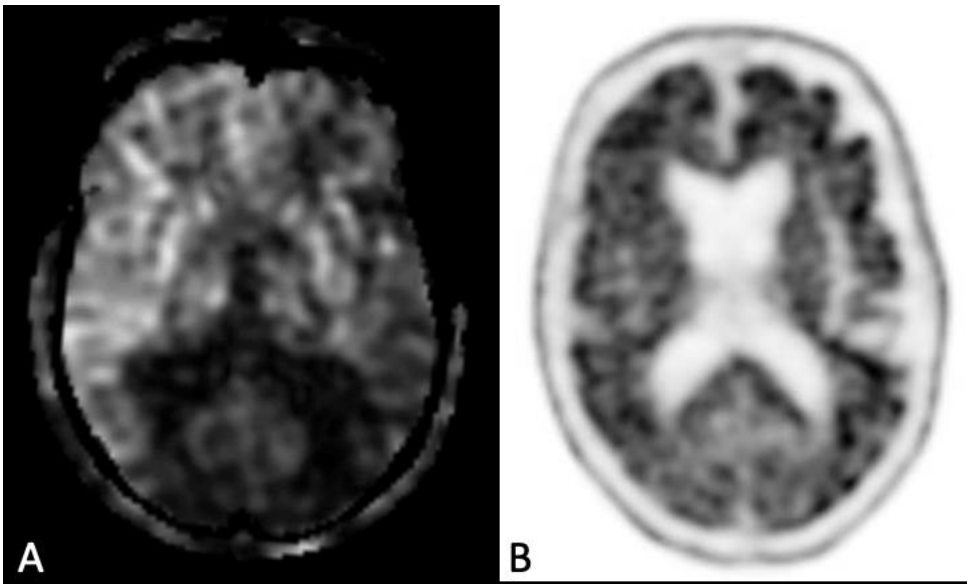

Supplementary Figure 23 (Case 6): (A) Gray-scale axial ASL-MR demonstrating decreased CBF in the bilateral parietal lobes (more pronounced on the left) and left frontal lobe, suggestive of neurodegenerative disease, particularly a primary progressive aphasia. **(B)** Axial [18F]-florbetaben PET image demonstrating diffuse cortical amyloid deposition, consistent with AD.

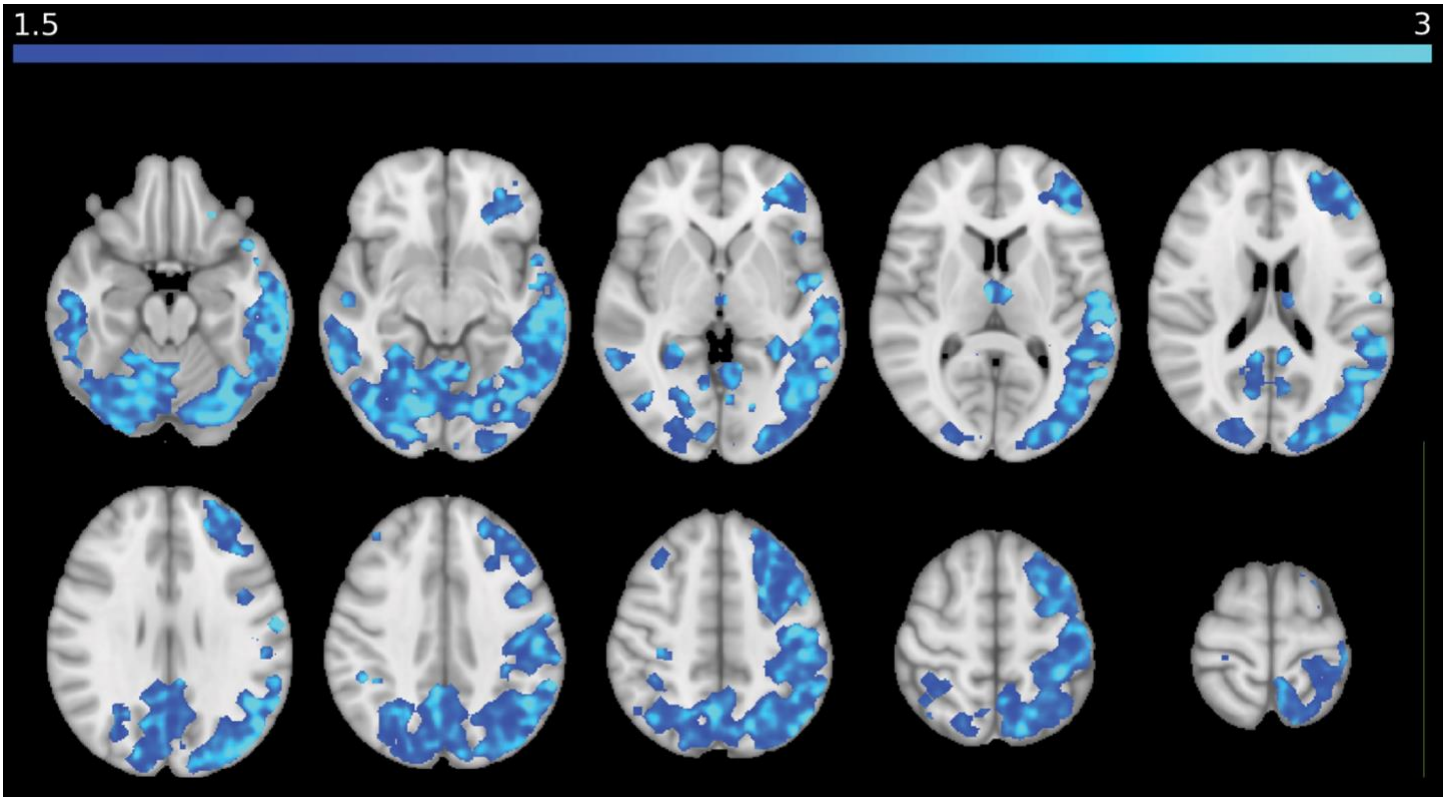

Supplementary Figure 24 (Case 6): Axial Z-score maps, with blue corresponding to areas of decreased CBF, predominantly in the temporal and parietal lobes, as well as the left frontal lobe. Upper and lower Z-score thresholds of 1.5 and 3.0 are shown in the color bar.

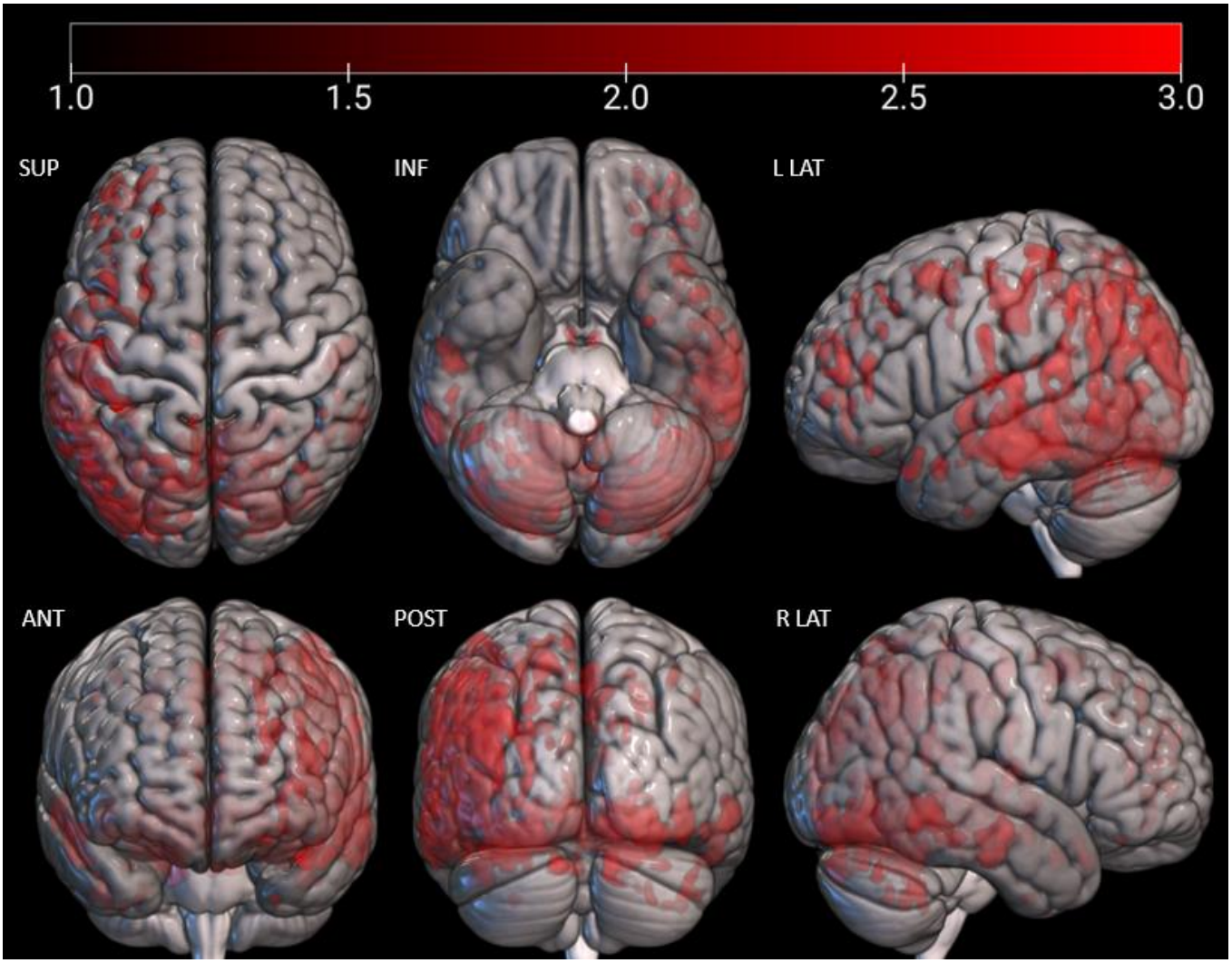

Supplementary Figure 25 (Case 6): Three-dimensional stereotactic surface projection images with red corresponding to decreased CBF, predominantly in the temporal and parietal lobes, as well as the left frontal lobe. Upper and lower Z-score thresholds of 1.0 and 3.0 are shown in the color bar.

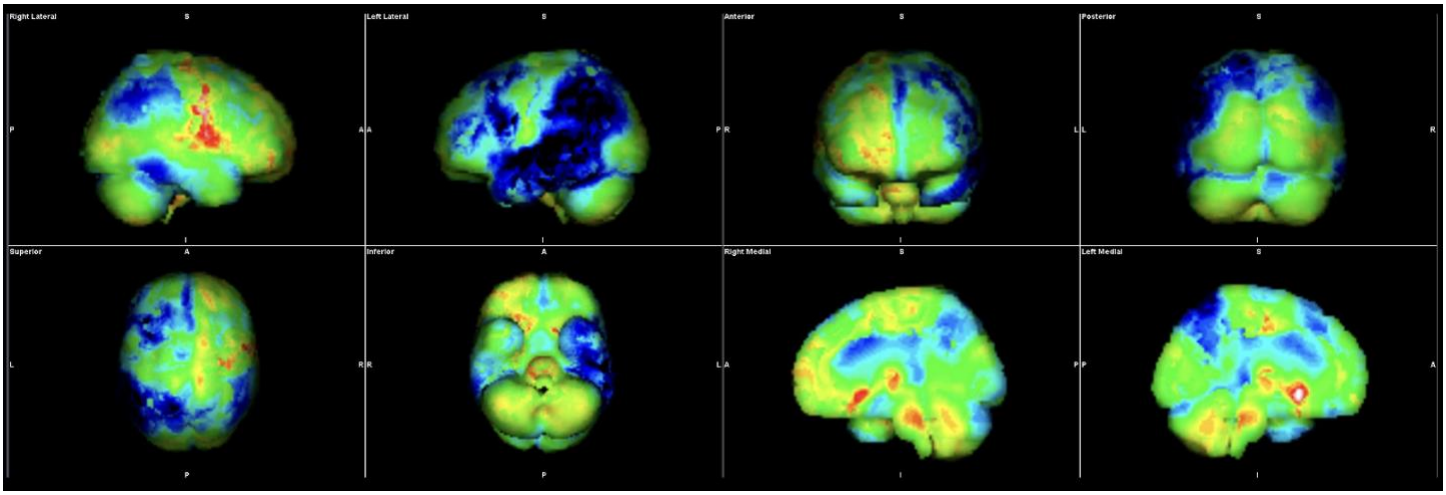

Supplementary Figure 26 (Case 6): Three-dimensional stereotactic surface projection images with blue representing the patient's decreased FDG avidity in the bilateral temporal and parietal lobes, as well as the left frontal lobe, using the clinically available syngo.via software package

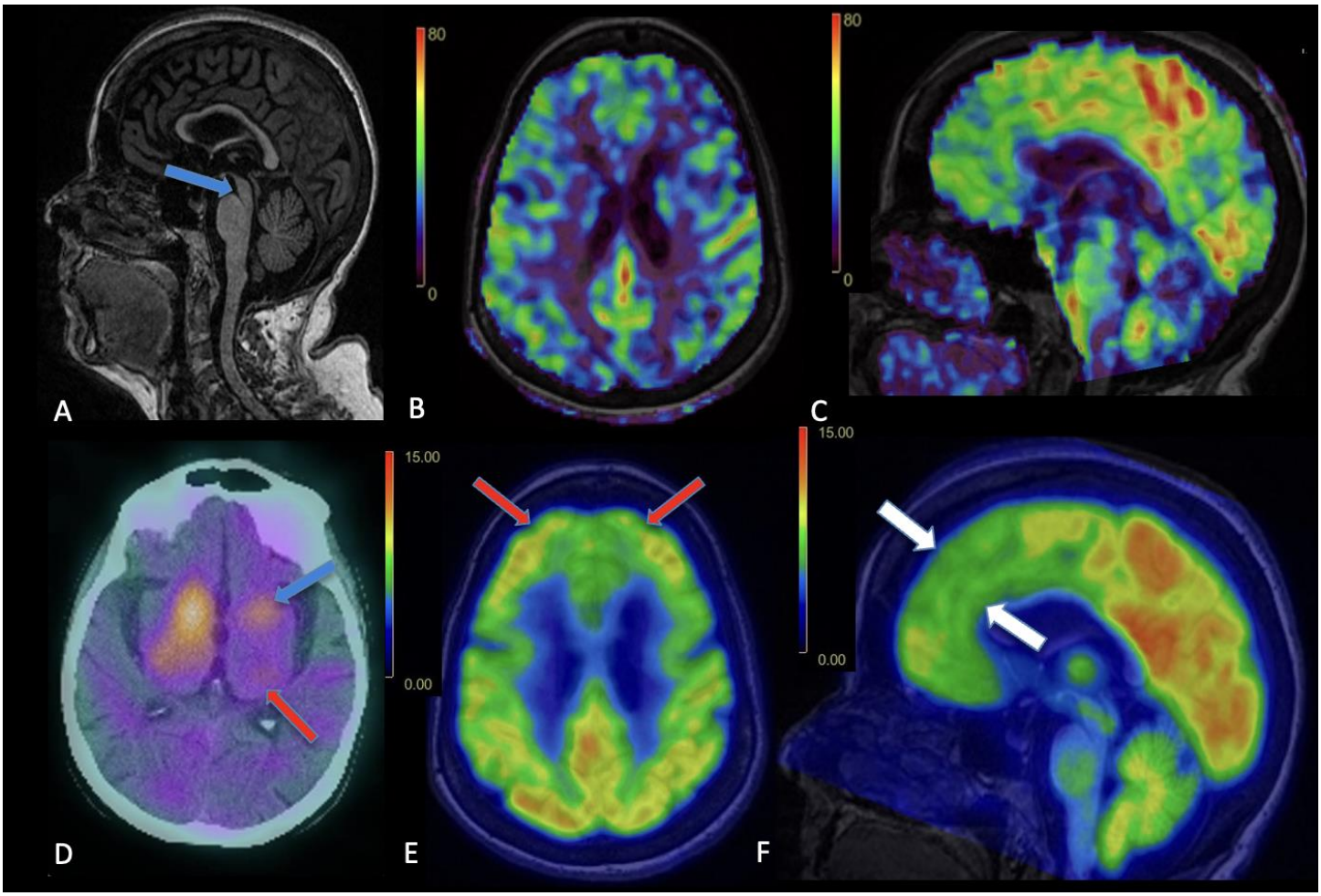

Supplementary Figure 27 (Case 7): Progressive Supranuclear Palsy. (A) Sagittal 3D T1 MPRAGE image showing midbrain atrophy (“hummingbird” sign) (blue arrow). Axial **(B)** and sagittal **(C)** CBF images showing decreased CBF in the bilateral frontal lobes, which was confirmed on axial **(E)** and sagittal **(F)** FDG-PET images. Axial image from a DaTscan **(D)** showing decreased radiotracer activity in the left caudate (blue arrow) and left (red arrow) greater than right putamina, supporting the diagnosis of progressive supranuclear palsy.

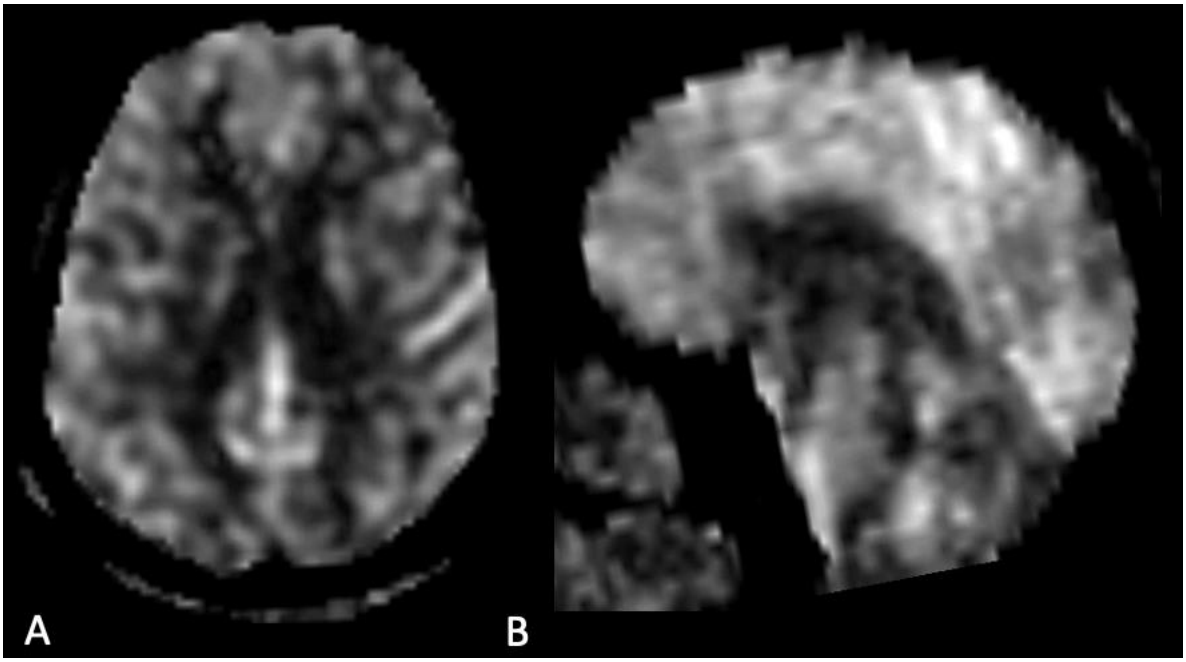

Supplementary Figure 28 (Case 7): Gray-scale axial and sagittal ASL-MR images demonstrating decreased CBF avidity predominantly in the bilateral frontal lobes (more pronounced on the left), suggestive of neurodegenerative disease.

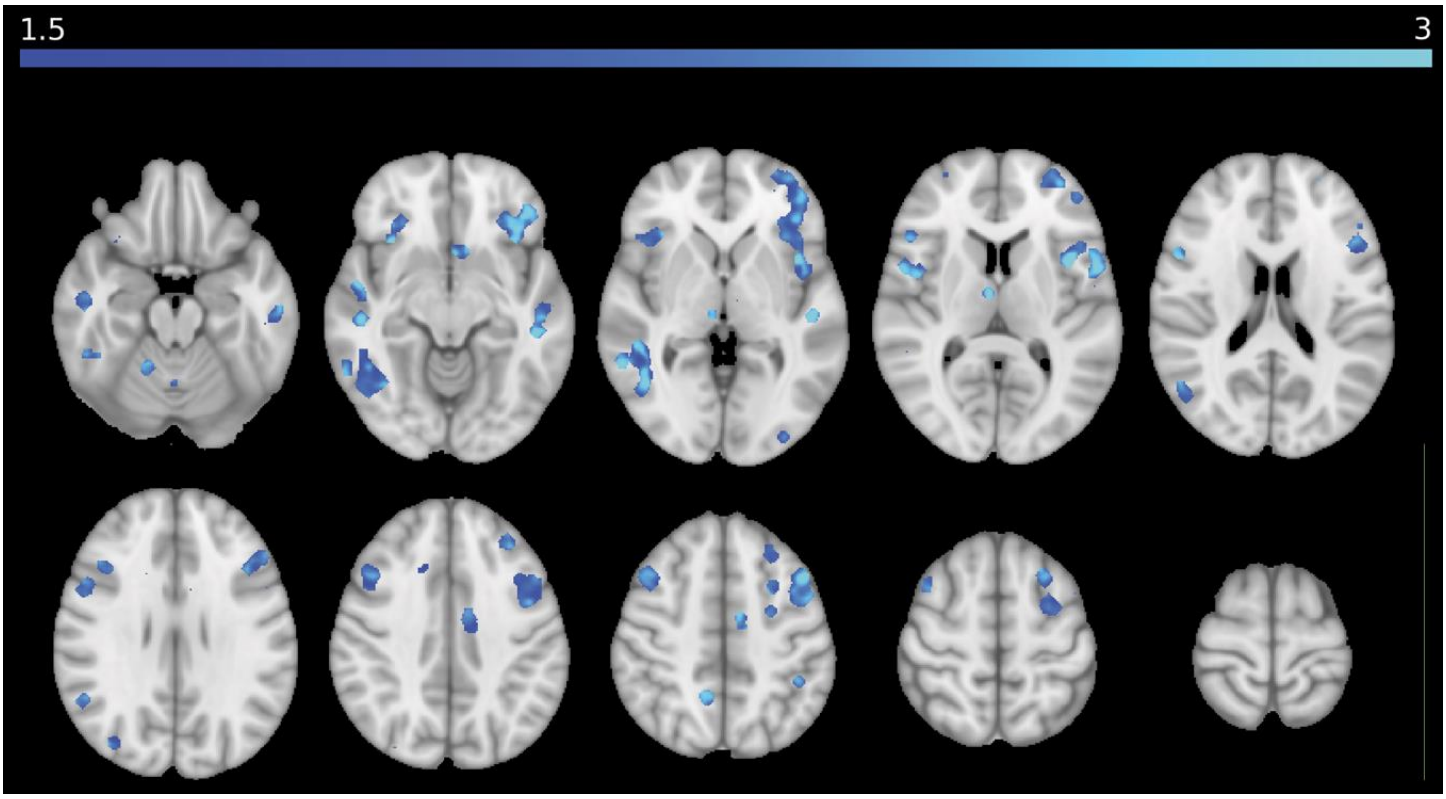

Supplementary Figure 29 (Case 7): Axial Z-score maps, with blue corresponding to areas of decreased CBF, predominantly in the frontal lobes. Upper and lower Z-score thresholds of 1.5 and 3.0 are shown in the color bar.

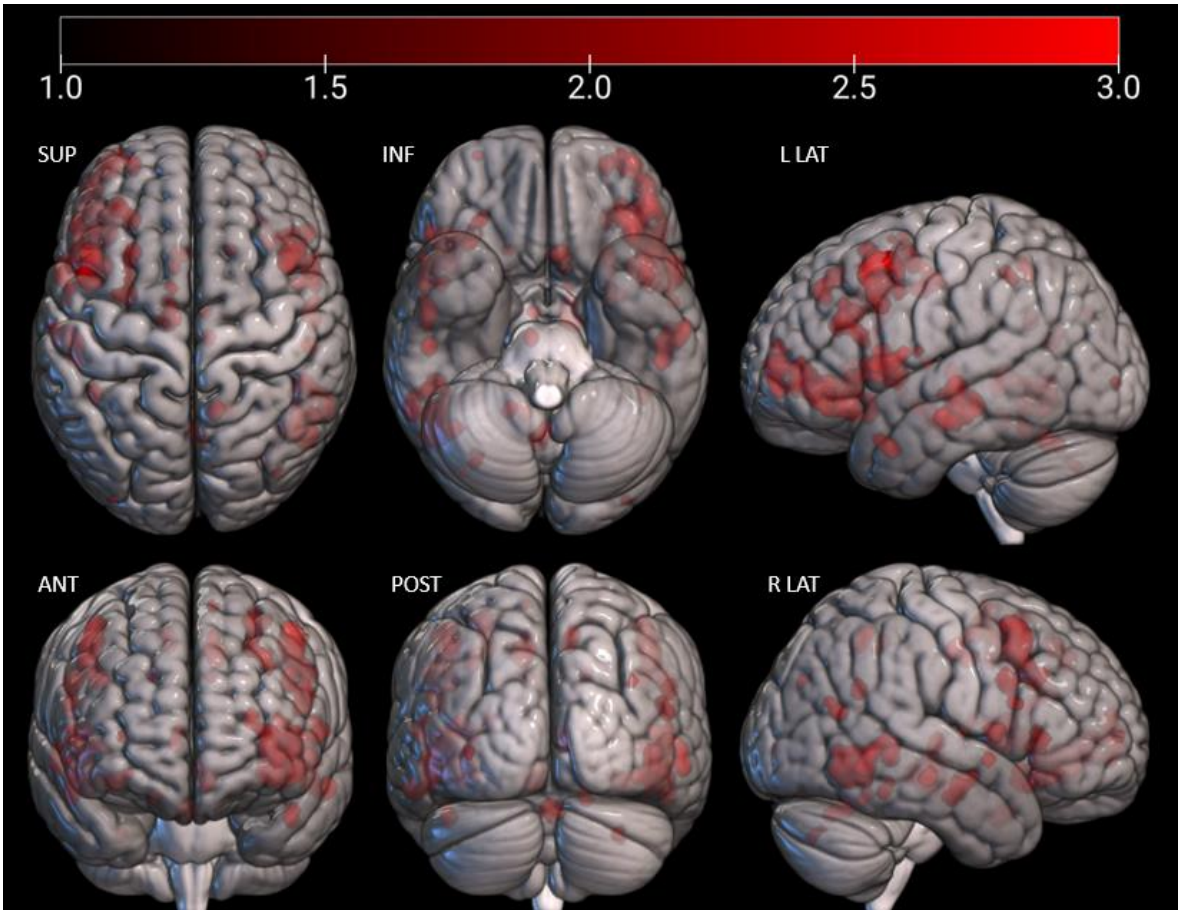

Supplementary Figure 30 (Case 7): Three-dimensional stereotactic surface projection images with red corresponding to decreased CBF, predominantly in the frontal lobes. Upper and lower Z-score thresholds of 1.0 and 3.0 are shown in the color bar.

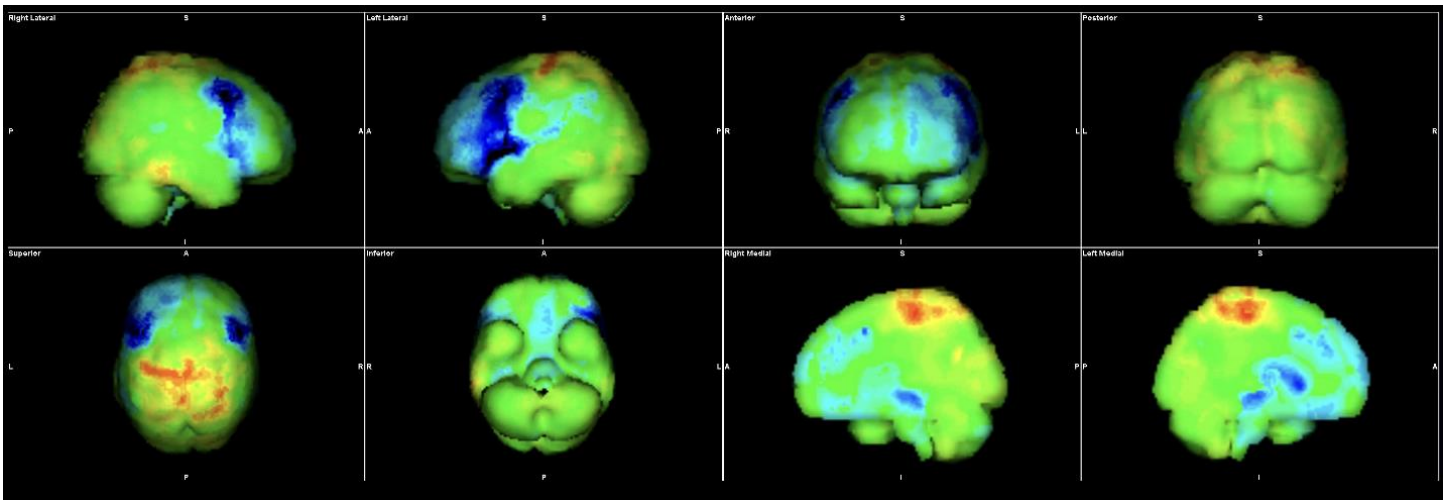

Supplementary Figure 31 (Case 7): Three-dimensional stereotactic surface projection images with blue representing the patient's decreased FDG avidity in the frontal lobes, using the clinically available syngo.via software package.